Article

Current Biology

Thermal-state-dependent control of body temperature and feeding by two intra-hypothalamic pathways

Graphical abstract

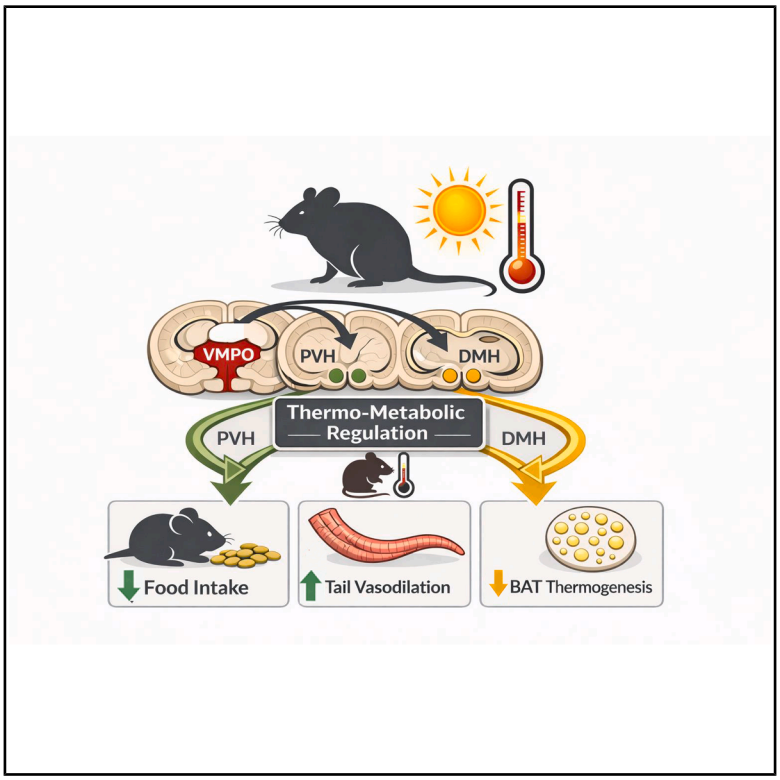

Authors

Hanan Bouaouda, Sara Nencini, Jan Siemens

Correspondence

jes@pharma.uni-heidelberg.de

In brief

Bouaouda et al. identify VMPO^{LepR} projections to the PVH and DMH as intra-hypothalamic circuits linking thermal state to energy balance. These pathways are required for thermoregulation under heat stress and influence feeding behavior.

Highlights

- VMPO^{LepR} neurons regulate body temperature and feeding via PVH and DMH pathways
- PVH and DMH projections exert distinct but complementary thermoregulatory roles
- Pathway inhibition causes hyperthermia, strongest under hot ambient conditions
- VMPO^{LepR}→PVH suppresses food intake more strongly at cool than warm temperatures

Bouaouda et al., 2026, Current Biology *36*, 1–15
March 9, 2026
https://doi.org/10.1016/j.cub.2026.01.074

CellPress

Current Biology

CellPress
OPEN ACCESS

Article

Thermal-state-dependent control of body temperature and feeding by two intra-hypothalamic pathways

Hanan Bouaouda,[1,3] Sara Nencini,[1,3,4] and Jan Siemens[1,2,5,*]
[1]Institute of Pharmacology, Heidelberg University, Im Neuenheimer Feld 366, 69120 Heidelberg, Germany
[2]Molecular Medicine Partnership Unit (MMPU), European Molecular Biology Laboratory (EMBL), Meyerhofstraße 1, 69117 Heidelberg, Germany
[3]These authors contributed equally
[4]Present address: Istituto Italiano di Tecnologia, via Morego 30, 16163 Genova, Italy
[5]Lead contact
*Correspondence: jes@pharma.uni-heidelberg.de
https://doi.org/10.1016/j.cub.2026.01.074

SUMMARY

The intricate interplay between energy metabolism and body temperature regulation underscores the necessity of finely tuned mechanisms to maintain thermo-energetic homeostasis. Hot environments are known to suppress food intake and to reduce energy expenditure. However, the interplay between thermoregulatory and caloric-regulatory hypothalamic areas remains largely unexplored. In this study, we unveil two pathways originating from a subpopulation of genetically defined leptin receptor-expressing ventromedial preoptic area (POA) neurons ($VMPO^{LepR}$) that connect to the paraventricular nucleus of the hypothalamus (PVH) and the dorsomedial hypothalamic nucleus (DMH). Both $VMPO^{LepR}$→PVH and $VMPO^{LepR}$→DMH pathways modulate brown adipose tissue (BAT) thermogenesis and body temperature, with their impact on body temperature regulation being particularly enhanced in a hot environment. Additionally, the pathways differentially regulate food intake and tail vasodilation, with feeding suppression being more prominent under cooler conditions and thermoregulatory effects more pronounced at elevated ambient temperatures. Our findings suggest that the $VMPO^{LepR}$→PVH and $VMPO^{LepR}$→DMH pathways integrate temperature and caloric information to complement the canonical inhibitory arcuate nucleus (ARC)→PVH pathway. We propose that these novel pathways contribute to energy and temperature homeostasis in hot environments, offering new insights into previously unrecognized neuronal circuits orchestrating thermo-metabolic balance in response to environmental challenges.

INTRODUCTION

Energy metabolism and body temperature are closely linked. In mammals, body temperature is usually maintained within a narrow range, requiring finely tuned heat-loss and heat-gain mechanisms that partially depend on energy utilization.[1,2] For example, cold ambient temperatures promote food consumption to meet energetic demands required for thermogenesis to keep the body warm. Conversely, warm ambient temperatures suppress food intake and energy expenditure, such as brown adipose tissue (BAT) thermogenesis, to maintain thermo-energetic homeostasis.[3–5]

The hypothalamus harbors neuronal centers that serve both regulatory processes, body temperature control and caloric balance. It has therefore been proposed that thermoregulatory and caloric-regulatory hypothalamic areas interact to coordinate energetic and thermal optimums,[6–9] and several cell populations modulating both feeding and body temperature have been characterized.[10–13] However, how different hypothalamic cell populations interact to govern the intricate thermo-metabolic balance and to resolve conflicting requirements and tradeoffs—for example, when scarcity of food prevents sustained thermogenesis in cold environments—is only partially understood.

Temperature information from peripheral (and central) thermoreceptors is integrated in the hypothalamic preoptic area (POA) to regulate body temperature via peripheral effector organs such as BAT, muscle, and skin blood vessels.[7,14–16]

The arcuate nucleus (ARC), on the other hand, is considered a main hub regulating energy homeostasis and contains interoceptive neurons responding to caloric state to regulate feeding behavior.[17,18] Several studies demonstrate that projections from the ARC to the paraventricular nucleus of the hypothalamus (PVH) are crucial for regulating caloric homeostasis and feeding.[19–22] However, only a few studies have implicated the PVH in body temperature regulation and BAT thermogenesis.[23–25] On the other hand, reciprocal thermo-metabolic connections have been suggested to exist between the POA and the ARC.[26,27] Moreover, recent data suggest that neuronal pathways from the POA to the PVH can influence feeding behavior.[26]

Please cite this article in press as: Bouaouda et al., Thermal-state-dependent control of body temperature and feeding by two intra-hypothalamic pathways, Current Biology (2026), https://doi.org/10.1016/j.cub.2026.01.074

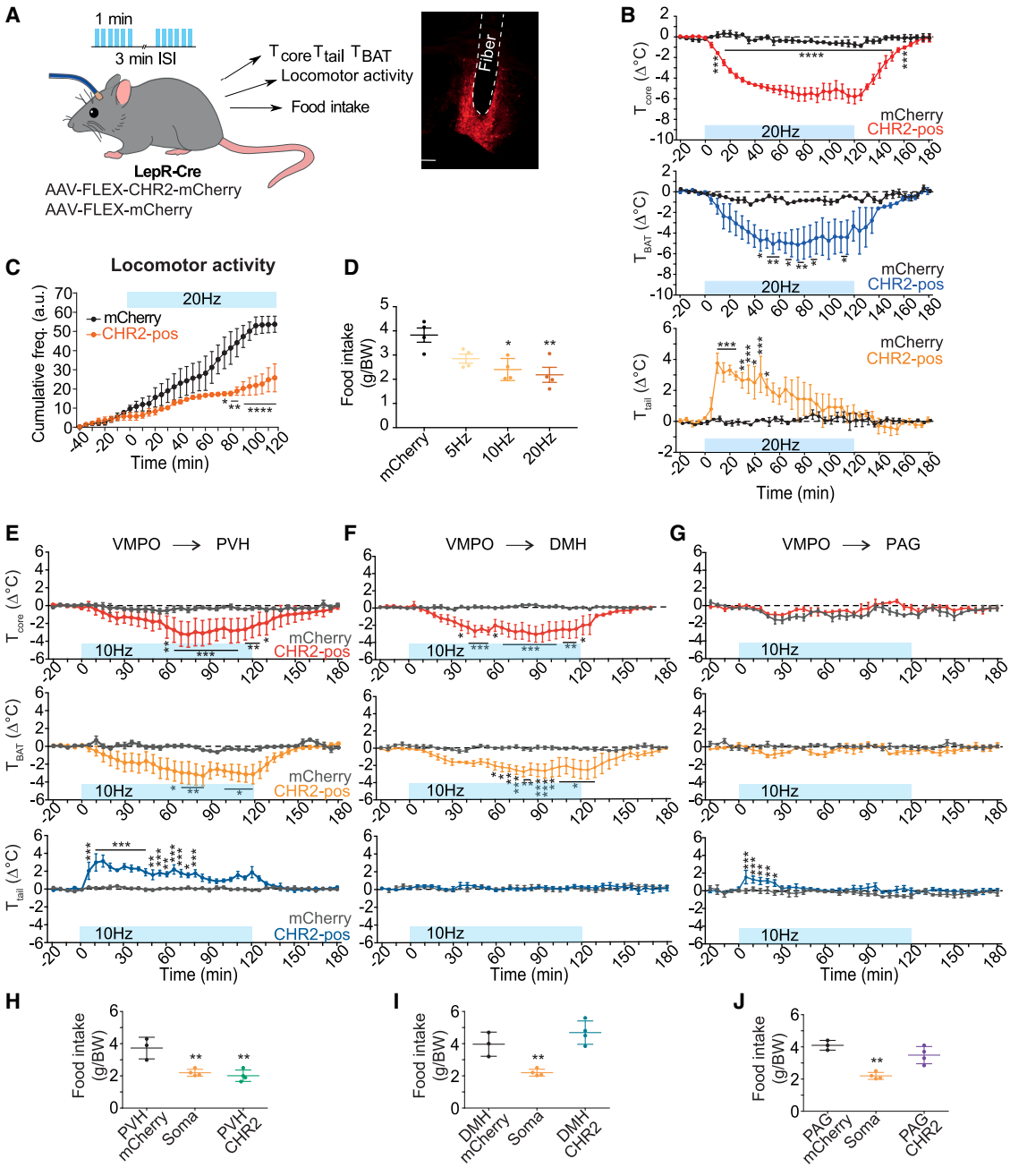

Figure 1. Optogenetic stimulation of VMPO^{LepR} neurons mediates body cooling and a reduction in food intake via PVH and DMH pathways

(A) Left: schematic of the optogenetic experiments. Optogenetic stimulation was applied unilaterally for 2 h using pulses of 10 ms duration (473 nm, max 6 mW) with varying stimulation frequencies (5, 10, and 20 Hz) for 1 min, followed by a 3 min inter-stimulation interval (ISI). Right: histological image showing optical fiber placement (white dotted line) and ChR2-mCherry expression in LepR cells in the VMPO area. Scale bar: 200 μm.

(B) Comparison between ChR2-positive and ChR2-negative (mCherry control) animals (n = 3 for each group) upon optogenetic stimulation. 20 Hz pulse stimulation decreased T_{core} (upper) as well as T_{BAT} (middle) while transiently increasing T_{Tai} (lower), specifically in ChR2-positive animals. The blue bar represents the time the light-pulse protocol was applied. Two-way ANOVA (effect of stimulation × time), $p < 0.0001$; Dunnett's multiple comparison test: *$p < 0.05$, **$p < 0.01$, ***$p < 0.001$, ****$p < 0.0001$.

(C) Mean cumulative locomotor activity (arbitrary units [a.u.]) of ChR2-positive and mCherry mice. Optogenetic stimulation reduced the locomotor activity. The blue bar represents the duration the light-pulse protocol was applied. Two-way ANOVA (effect of stimulation x time), $p < 0.0001$, Dunnett's multiple comparison test: *$p < 0.05$, **$p < 0.01$, ***$p < 0.001$ (n = 3 mice per group).

(D) Food intake was significantly suppressed in ChR2-positive animals upon light activation, compared with mCherry (n = 4 mice for each group) with light stimulation performed overnight. One-way ANOVA; Dunnett's multiple comparison test: *$p < 0.05$, **$p < 0.01$ versus mCherry group.

(legend continued on next page)

Please cite this article in press as: Bouaouda et al., Thermal-state-dependent control of body temperature and feeding by two intra-hypothalamic pathways, Current Biology (2026), https://doi.org/10.1016/j.cub.2026.01.074

Circulating leptin serves as an indicator of energy status,[28] and the hormone also plays a major role in body temperature regulation.[29] Interestingly, leptin receptor-positive neurons in the rostral part of the POA, the so-called ventromedial POA (VMPO), are warm-responsive neurons activated by ambient temperature increases that modulate both body temperature and food consumption. Specifically, activating these neurons *in vivo* triggers profound hypothermia and inhibits food intake.[13,30,31] However, the neural pathways that these thermoregulatory neurons utilize to precisely regulate food intake in accordance with thermo-metabolic balance and body temperature stability remain elusive.

We here describe two pathways that originate from a population of leptin receptor-expressing POA neurons ($VMPO^{LepR}$ neurons) that inhibit feeding and diminish BAT thermogenesis by targeting the PVH and dorsomedial hypothalamic nucleus (DMH). $VMPO^{LepR}$ neurons do not exclusively target the PVH and DMH, and we also find connections to the periaqueductal gray (PAG) and the ARC. However, monosynaptic connections of $VMPO^{LepR}$ neurons to the PVH and DMH appear to be unique in that they orchestrate inhibition of food intake and BAT thermogenesis while simultaneously also mediating heat-loss mechanisms.

We propose that the $VMPO^{LepR}$→PVH and $VMPO^{LepR}$→DMH loops integrate temperature and energy-metabolic information to complement and fine-tune the well-established inhibitory ARC→PVH pathway, thereby conjointly achieving energy and temperature homeostasis in hot environments.

RESULTS

Excitatory $VMPO^{LepR}$ neurons promote hypothermia and inhibit food intake

To investigate the impact of $VMPO^{LepR}$ neuron activity on body temperature, we photostimulated LepR cell bodies using optic fibers implanted unilaterally above the VMPO (Figure 1A). Light stimulation at frequencies of 5 Hz or higher produced electrophysiological responses in *ex vivo* slice preparations and resulted in a drop in body temperature (T_{core}) in a frequency-graded fashion (Figures S1A and S1B). This coincided with a drop in BAT temperature (T_{BAT}) and a transient increase in tail temperature indicative of cutaneous vasodilation (Figures 1B and S1C). Additionally, we observed a decrease in overall ambulatory activity and a suppression of food intake in mice expressing channelrhodopsin-2 (ChR2) in $VMPO^{LepR}$ neurons (Figures 1C and 1D). These thermoregulatory and energy-metabolic responses were dependent on ChR2 expression and were not observed in (mCherry-expressing) control animals. Furthermore, these responses appeared to be independent of the hypothalamic-pituitary-adrenal axis, as corticosterone levels remained at baseline levels (Figure S1D).

These findings corroborate and expand on previous observations from chemogenetic and optogenetic manipulation experiments.[13,31]

A $VMPO^{LepR}$→PVH pathway suppresses feeding and promotes body cooling

We next asked which target areas downstream of $VMPO^{LepR}$ neurons mediate thermoregulatory and feeding responses and whether the two functionalities are controlled by separate pathways. The POA is connected to several hypothalamic and extrahypothalamic brain areas, with POA fibers prominently innervating the ventrolateral septal area (LSV), the bed nucleus of the stria vascularis (BNST), the ARC, the paraventricular thalamus (PVT), the medial habenula (mHB), the raphe pallidus (RP), the ventrolateral PAG (vlPAG), the dorsomedial hypothalamus (DMH), and the paraventricular hypothalamus (PVH).[32] All of these regions have been implicated in the control of feeding,[33–35] while the DMH and, to a lesser extent, also the vlPAG have been additionally implicated in thermoregulation.[7,36] We found fiber terminals of $VMPO^{LepR}$ neurons to intensely innervate the PVH and DMH, and to a lesser extent we observed fiber labeling also in the PAG (Figures S2A–S2C). Particularly, the PVH was robustly and strongly innervated by $VMPO^{LepR}$ neuron fibers (Figure S2D). We therefore focused on the PVH, DMH, and PAG as potential relay stations for thermoregulatory and feeding-regulatory $VMPO^{LepR}$ neuron projections.

To assess the role of $VMPO^{LepR}$ projections innervating these 3 target areas, we again used an optogenetic approach by virally expressing ChR2 in $VMPO^{LepR}$ neurons and directing the light source to the different target areas in order to selectively stimulate fiber terminals in the DMH, PAG, or PVH (Figure S2E).

While activating projections innervating the PAG did not have any significant influence on body temperature, those innervating the DMH and PVH both decreased body temperature, likely via inhibiting BAT thermogenesis (Figures 1E–1G). Projections to PVH, but not those innervating the DMH, additionally mediated transient tail vasodilation (Figures 1E and 1F). Activating the $VMPO^{LepR}$→PVH pathway overnight significantly reduced food intake, similar to activating the $VMPO^{LepR}$ cell bodies (somatic activation), while activating terminals in the DMH and PAG had no apparent effect on food intake (Figures 1H–1J).

Because projections to the DMH and PVH had overlapping (but not identical) functionalities in the context of thermoregulation,

(E) Optogenetic stimulation (10 Hz) of $VMPO^{LepR}$ terminals in the PVH of ChR2 mice ($n = 5$) decreased T_{core} and T_{BAT} and increased T_{Tail} versus mCherry controls ($n = 5$). Two-way ANOVA (effect of stimulation × time), $p < 0.0001$ for T_{core}, T_{BAT}, and T_{Tail}.
(F) Stimulation of $VMPO^{LepR}$ terminals in the DMH ($n = 4$) decreased T_{core} and T_{BAT} but not T_{Tail} versus controls ($n = 4$). Two-way ANOVA (effect of stimulation × time), $p < 0.0001$ for T_{core} and T_{BAT}.
(G) Stimulation of $VMPO^{LepR}$ terminals in the PAG ($n = 3$) did not alter T_{core}, T_{BAT}, or T_{Tail} versus controls ($n = 3$).
The blue bar indicates the light-stimulation period. Dunnett's test: $^{*}p < 0.05$, $^{**}p < 0.01$, $^{***}p < 0.001$, $^{****}p < 0.0001$.
(H–J) Food consumption normalized to body weight during overnight optogenetic stimulation of VMPO(LepR) cell bodies ("LepR soma") or their PVH (H), DMH (I), and PAG (J) projection sites (PVH-, DMH-, and PAG-ChR2). Light-stimulated control animals expressed mCherry in the corresponding projection sites (PVH-, DMH-, and PAG-mCherry). Note that food intake was significantly suppressed when LepR to PVH (but not LepR to DMH or PAG) projections were light activated. One-way ANOVA, $^{**}p < 0.01$. $n = 4$ mice for soma, PVH, DMH, and PAG groups; $n = 3$ mice for control groups; note that the LepR soma data (somatic activation) is partially overlapping with data shown in Figure 3F.
Data in (B–J) are shown as mean ± SEM.
See also Figures S1–S3.

Please cite this article in press as: Bouaouda et al., Thermal-state-dependent control of body temperature and feeding by two intra-hypothalamic pathways, Current Biology (2026), https://doi.org/10.1016/j.cub.2026.01.074

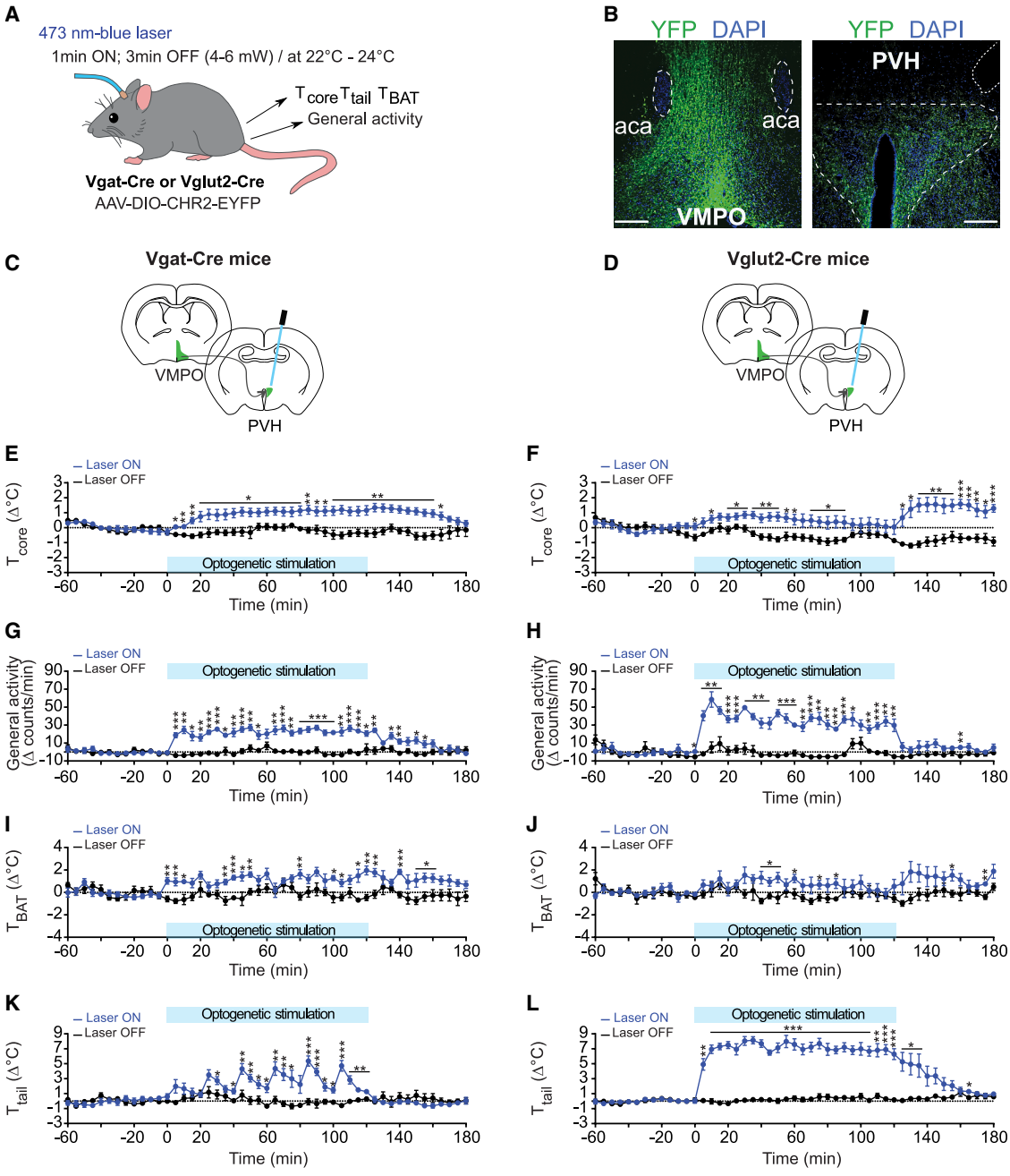

Figure 2. Optogenetic stimulation of VMPO^{Vgat}→PVH and VMPO^{Vglut2}→PVH terminals increases body temperature, tail vasodilatation, and general locomotor activity

(A) Schematic summarizing the optogenetic experiments. Optogenetic stimulation was applied unilaterally for 2 h during the light phase at 22°C–24°C room temperature, using pulses of 10 ms duration (473 nm, max 6 mW) with a stimulation frequency of 10 Hz for 1 min, followed by a 3-min inter-stimulation interval (ISI).
(B) Histological images showing ChR2-EYFP fluorescence in the Vglut2-positive (glutamatergic) cells in the VMPO (left) and their terminals innervating the PVH (right, PVH area demarcated by dashed white line). Scale bar: 200 μm.
(C) Schematic showing AAV-ChR2 injection into the VMPO and implantation of an optic fiber above the PVH in Vgat-Cre mice (n = 5).
(D) Schematic showing AAV-ChR2 injection into the VMPO and implantation of an optic fiber above the PVH in Vglut2-Cre mice (n = 5).
(E) Time course of T_{core} from the same cohort of Vgat-Cre mice measured on a non-stimulated day (laser OFF, black trace) and the subsequent day during optogenetic stimulation (laser ON, blue trace).
(F) Time course of T_{core} from the same cohort of Vglut2-Cre mice measured on a non-stimulated day (laser OFF, black trace) and the subsequent day during optogenetic stimulation (laser ON, blue trace).
(G) Time course of general locomotor activity of Vgat-Cre mice during optogenetic stimulation (laser ON, blue trace) or control condition (laser OFF, black trace).
(H) Time course of general locomotor activity of Vglut2-Cre mice during optogenetic stimulation (laser ON, blue trace) or control condition (laser OFF, black trace).
(I) Time course of T_{BAT} of Vgat-Cre mice during optogenetic stimulation (laser ON, blue trace) or control condition (laser OFF, black trace).

(legend continued on next page)

Please cite this article in press as: Bouaouda et al., Thermal-state-dependent control of body temperature and feeding by two intra-hypothalamic pathways, Current Biology (2026), https://doi.org/10.1016/j.cub.2026.01.074

while only PVH projections suppressed food intake, we assessed to what extent VMPO^{LepR} neurons innervating the PVH and DMH overlap. Injecting retroAAV particles into the DMH and PVH of LepR-Cre animals permitted the infection of fiber terminals to label upstream VMPO^{LepR} neurons with Cre-recombinase-dependent red and green fluorophores, respectively. We found that only a small fraction of neurons overlapped, suggesting that collateralization to both areas is limited, and the larger fraction of VMPO^{LepR} neurons appeared to project to either the PVH or the DMH (Figure S3).

Vglut2-positive, presumed excitatory VMPO^{LepR} projections to the PVH and DMH mediate thermoregulatory and feeding responses

Warm-responsive VMPO^{LepR} neurons encompass both excitatory (Vglut2-positive) and inhibitory (Vgat-positive) neurons.[13] Although still controversial,[37,38] previous results suggested that excitatory POA neurons play a more prominent role in modulating body temperature than previously anticipated.[14,30,39–41] We therefore employed Vglut2-Cre and Vgat-Cre mouse lines to assess if VMPO^{Vglut2}→PVH and/or VMPO^{Vgat}→PVH pathways recapitulate the above findings (Figures 2A–2D and S4A–S4C).

Surprisingly, optogenetically stimulating Vglut2-positive (excitatory) or Vgat-positive (inhibitory) fiber terminals innervating the PVH resulted in an increase in body temperature rather than a decrease (Figures 2E and 2F), an effect that was less pronounced at night (Figures S4D and S4E). Strong induction of locomotor activity explained the T_{core} increase, at least partially (Figures 2G, 2H, and S4F–S4H), which in the case of VMPO^{Vglut2}→PVH terminal activation had the appearance of escape responses (Video S1), while in the case of the VMPO^{Vgat}→PVH pathway, it presented as foraging activity that was interrupted by feeding bouts in the periods laser stimulation was off (Video S2). In agreement with these observations, overnight food intake increased when activating the VMPO^{Vgat}→PVH, but not the VMPO^{Vglut2}→PVH, pathway (Figures S4I and S4J). In parallel, heat production via BAT thermogenesis (Figures 2I and 2J) and heat dissipation (Figures 2K, 2L, and S4K) were simultaneously active, the latter presenting as strong continuous tail vasodilatatory activity in the case of VMPO^{Vglut2}→PVH activation and episodic tail vasodilation in the case of VMPO^{Vgat}→PVH activation. These results suggest that indiscriminately activating broad populations of excitatory or inhibitory fiber terminals innervating the PVH has multiple thermoregulatory and behavioral effects. We hypothesized that in sum these—partially opposing—thermoregulatory effects masked the body cooling response observed when activating VMPO^{LepR}→PVH pathways. Interestingly, subsequent to optogenetic stimulation of VMPO→PVH fiber terminals, T_{core} increased in Vglut2-Cre animals but not in Vgat-Cre animals (Figures 2E and 2F). This observation agrees with the notion that both heat-producing and heat-loss mechanisms may be engaged during Vglut2-positive fiber stimulation, partially offsetting their individual effects on T_{core}. After termination of optogenetic stimulation, different relaxation times of these thermo-effector responses may have produced a transient net increase in T_{core}.

We therefore utilized an intersectional approach to specifically investigate the impact of excitatory or inhibitory VMPO^{LepR} neurons—and their projections to PVH and DMH—on thermoregulatory responses and feeding. To achieve this goal, we employed LepR-Cre;Vgat-FlpO mice in combination with adeno-associated viruses (AAVs) that enable ChR2 expression in a Cre- and FlpO-dependent manner (Figure 3A). With this approach, we did not target the excitatory (Vglut2-positive) population directly but activated either inhibitory (Vgat-FlpO-on) or non-inhibitory (Vgat-FlpO-off) VMPO^{LepR} neurons, presuming that the Vgat-FlpO-off VMPO^{LepR} population is largely comprised of excitatory neurons. For simplicity, we hereafter refer to these populations as vGat.LepR (GABAergic) and non-vGat.LepR (non-GABAergic) neurons.

We first confirmed in *ex vivo* brain slice preparations that optical stimulation, using different light-pulse frequencies (5, 10, and 20 Hz), triggers corresponding action-potential frequencies in ChR2-expressing neurons. This experiment showed that both vGat.LepR and non-vGat.LepR neurons could sustain stimulation frequencies of up to 10 Hz but that inhibitory neurons did not faithfully recapitulate 20 Hz optical stimulation frequencies (Figures 3B–3E). These results are in agreement with previous findings showing that galanin-positive POA neurons, which are predominantly inhibitory, similarly failed to respond to higher stimulation frequencies.[42]

At optic stimulation frequencies that are compatible with triggering tonic action potentials in excitatory and inhibitory neurons, we find that non-vGat.LepR neurons inhibited BAT thermogenesis, transiently activated cutaneous vasodilation, and suppressed food intake (Figures 3F and 3G). Optic activation of vGat.LepR neurons only resulted in a subtle drop in food intake and less pronounced responses in thermogenesis and tail vasodilation (Figures 3F and 3H). These results agree with previous studies, targeting preoptic Vglut2-expressing excitatory neurons non-selectively.[13,26,41]

Next, we assessed the impact of stimulating the corresponding fiber terminals in the PVH and DMH. Optogenetically activating excitatory but not inhibitory VMPO^{LepR} projections to PVH, and to a lesser extent DMH, recapitulated BAT inhibition and hypothermia induction (Figures 4A–4D). Activating the PVH projections also induced transient tail vasodilation (Figure 4A). Inhibition of food intake was most robustly observed when activating excitatory VMPO^{LepR} projections to the PVH. Subtle inhibition of food intake was also revealed when activating vGAT-positive inhibitory terminals innervating the DMH (Figures 4E and 4F).

Collectively, these results suggest that independent parallel pathways to the PVH and DMH, originating largely from excitatory (Vglut2-positive) VMPO^{LepR} neurons, regulate body

(J) Time course of T_{BAT} of Vglut2-Cre mice during optogenetic stimulation (laser ON, blue trace) or control condition (laser OFF, black trace).
(K) Time course of T_{Tail} of Vgat-Cre mice during optogenetic stimulation (laser ON, blue trace) or control condition (laser OFF, black trace).
(L) Time course of T_{Tail} of Vglut2-Cre mice during optogenetic stimulation (laser ON, blue trace) or control condition (laser OFF, black trace).
Each data point corresponds to mean ± SEM. Data were recorded every 5 min. Repeated-measures two-way ANOVA followed by post hoc Fisher's least significant difference (LSD) tests were performed. The blue bars indicate the time window of light-pulse stimulation.
Asterisks indicate a statistically significant difference (*$p < 0.05$, **$p < 0.01$, ***$p < 0.001$).
See also Figure S4 and Videos S1 and S2.

Please cite this article in press as: Bouaouda et al., Thermal-state-dependent control of body temperature and feeding by two intra-hypothalamic pathways, Current Biology (2026), https://doi.org/10.1016/j.cub.2026.01.074

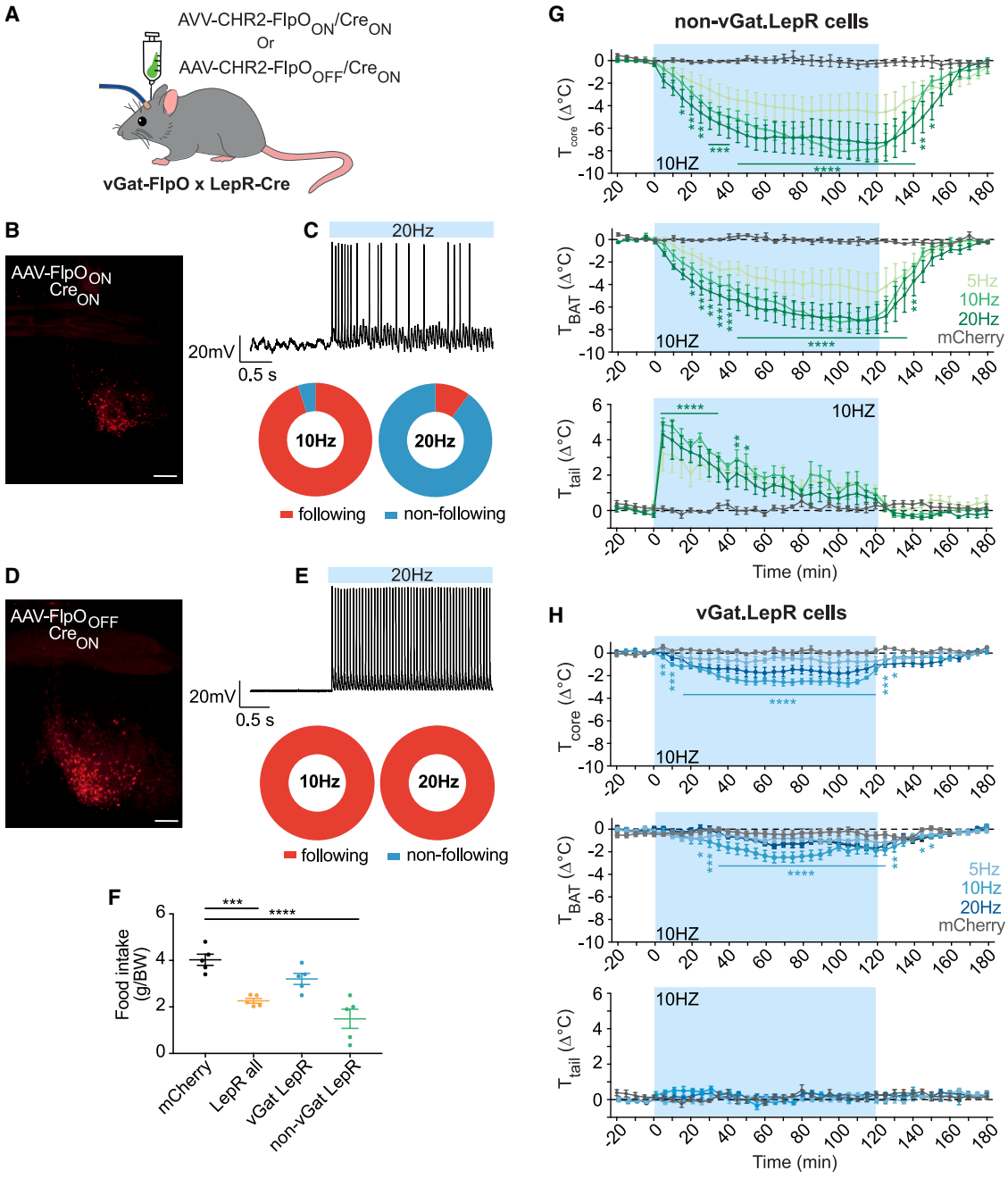

Figure 3. Predominantly VGAT-negative VMPO^{LepR} neurons drive hypothermia and reduction in food intake

(A) Schematic of the intersectional AAV strategy to express ChR2 in vGat.LepR or non-vGat.LepR VMPO neurons in Vgat-FlpO × LepR-Cre mice.

(B and D) Representative histological images of the VMPO region showing expression of rAAV(DJ)-Cre(ON)/FlpO(ON)-ChR2 virus and rAAV(DJ)-Cre(ON)/FlpO(OFF)-ChR2 virus, respectively. Scale bar 200 μm.

(C and E) Upper: example traces of action-potential response evoked by blue light stimulation at 20 Hz stimulation frequency in FlpO$_{ON}$, Cre$_{ON}$ brain slices (C) or FlpO$_{OFF}$, Cre$_{ON}$ brain slices (E). The blue bar denotes the period during which light pulses were delivered. Lower: pie charts showing the percentage of neurons that were able (following) or not able (non-following) to induce action potentials at the same frequency as the indicated light stimulation frequency in electrophysiological *ex vivo* brain slice recordings. Note that stimulation at 20 Hz (in contrast to 10 Hz stimulation frequency) failed to consistently elicit action potentials in the majority of the vGat-positive LepR neuronal population.

(F) Overnight (10 Hz) stimulation of non-vGat LepR cells significantly suppressed food intake, comparable to stimulating the whole LepR population ("LepR all"; note that this data is partially overlapping with LepR soma data shown in Figure 1H; $n = 5$ mice for each group). One-way ANOVA; Dunnett's multiple comparison test: $^{**}p < 0.01$, $^{***}p < 0.001$.

(legend continued on next page)

Please cite this article in press as: Bouaouda et al., Thermal-state-dependent control of body temperature and feeding by two intra-hypothalamic pathways, Current Biology (2026), https://doi.org/10.1016/j.cub.2026.01.074

temperature by inhibiting BAT thermogenesis and inducing tail vasodilation, while food intake appears to be differentially regulated via excitatory and inhibitory VMPO^{LepR}→PVH and VMPO^{LepR}→DMH projections, respectively.

Hot ambient temperatures enhance the contribution of the VMPO^{LepR}→PVH/DMH pathways to body temperature regulation

Our optogenetic stimulation experiments did not allow us to determine under which physiological conditions the identified pathways might be functionally relevant.

The POA, including the VMPO, is known to integrate thermal information for body temperature homeostasis. It has been shown that VMPO^{LepR} neurons are activated by hot temperatures to mediate body cooling.[13,31,43] We therefore wondered whether the identified VMPO^{LepR}→PVH/DMH pathways might regulate body temperature and/or food intake under hot environmental conditions.

To address this question, and in order to inhibit neurotransmitter release from fiber terminals at different environmental temperatures, we employed the inhibitory opsineOPN3 (enhanced mosquito homolog of the vertebrate encephalopsin).[44–46] This opsin has been shown to effectively inhibit transmitter release when activated by blue to green light.[46]

We first assessed the effect on T_{core} and food intake when inhibiting VMPO^{LepR} terminals innervating the PVH and DMH under basal ("room temperature," 22°C–24°C) conditions. When comparing eOPN3-expressing animals with control animals, inhibition of either pathway resulted in a subtle but statistically significant increase in T_{core} (Figures 5A–5D and S5). For the VMPO^{LepR}→PVH pathway, this effect appeared to be mediated, at least in part, by a small increase in T_{BAT} (Figures 5E, 5F, S6A, and S6B). General locomotor activity appeared not to be altered by the stimulation in either the DMH or PVH group (Figures 5G and 5H). We did not observe any tail vasoconstriction, which in principle could contribute to the T_{core} increase (Figures 5I, 5J, S6A, and S6B). This is likely because, at room temperature, the blood vessels in the mouse tail are already largely constricted, preventing further constriction upon inhibition of potentially permissive VMPO^{LepR}→PVH/DMH pathways.

Inhibiting either pathway by activating eOPN3 overnight had similar effects on body temperature and locomotor activity compared with daytime inhibition, and, again, T_{core} was slightly elevated when both pathways were inhibited, without affecting general locomotor activity (Figures S6C–S6J). Importantly, inhibiting either of the two (VMPO^{LepR}→PVH/DMH) pathways significantly increased food intake (Figures 5K and 5L). These results (increased T_{core} and food intake) are consistent with our ChR2-mediated optogenetic activation experiments (decreased T_{core} and food intake; Figures 1E, 1F, and 1H). Together, the data suggest that both pathways are, at least partially, engaged under basal ambient temperature conditions (22°C–24°C).

Next, we acutely exposed the mice to hot temperatures (36°C) and inhibited the VMPO^{LepR}→PVH/DMH pathways under these conditions. Interestingly, the T_{core} of eOPN3-inhibited mice increased robustly compared with control mice when either the VMPO^{LepR}→PVH or the VMPO^{LepR}→DMH pathway was inhibited (Figures 6A–6C). Again, inhibition did not measurably affect general locomotor activity (Figures 6D and 6E). In this short-term heat challenge experiment (5 h), which was conducted during the day/light phase, we did not measure food intake because mice are nocturnal and consume most of their food during the dark phase.

We recently implicated VMPO^{LepR} neurons also in long-term heat acclimation and as mediators of heat tolerance.[31]

To assess whether VMPO^{LepR}→PVH/DMH pathways modulate food intake and body temperature during long-term heat exposure, we performed a heat-acclimation experiment in which animals were conditioned to 36°C for 4 weeks. Inhibiting either pathway via eOPN3 stimulation at the end of the acclimation phase resulted in robust hyperthermia during both the light and dark phases, without affecting general locomotor activity (Figures 6F–6I and S7). When assessing overnight food intake, we observed a small but significant increase only upon inhibition of the VMPO^{LepR}→PVH pathway but not the VMPO^{LepR}→DMH pathway (Figures 6J and 6K). These findings mirror our optogenetic activation experiments, which showed that engagement of the VMPO^{LepR}→PVH pathway—but not the VMPO^{LepR}→DMH pathway—suppresses overnight feeding (Figures 1H and 1I).

Lastly, we asked whether the effect of the two VMPO pathways on body temperature becomes more pronounced at warm ambient temperatures, given that VMPO^{LepR} neurons have been shown to be activated by heat. It has been suggested that eOPN3 is highly sensitive to light[46] and may even exhibit subtle baseline activity without optical stimulation due to light penetration through the mouse skull and brain.[47] This may explain the slightly higher body and BAT temperatures of eOPN3-expressing mice even before fiber optic light stimulation when compared with control animals (Figures 5E, 6B, 6C, 6F, 6G, S6G, S7H, and S7I).

Because this background activity complicates direct comparisons with control animals not expressing eOPN3, we quantified the thermal impact within eOPN3-expressing mice by calculating the area under the T_{core} curve (AUC)—a measure of cumulative heat load—across ambient conditions (22°C–24°C versus acute 36°C versus acclimated 36°C). While inhibition of either pathway had only minor effects at room temperature, either pathway induced robust hyperthermia during both acute and prolonged heat exposure (Figure 7). Collectively, these findings indicate that the VMPO^{LepR}→PVH/DMH pathways are critical for maintaining thermal balance and preventing overheating in hot environments.

Moreover, the VMPO^{LepR}→PVH pathway suppresses food intake under both temperate and hot ambient conditions, albeit more effectively at cooler conditions.

(G) Optogenetic stimulation of VMPO vGat-negative LepR neurons reduced T_{core} and T_{BAT} and transiently increased T_{Tail} in ChR2 mice, but not in mCherry controls, across all stimulation frequencies (n = 5/group). Two-way ANOVA (effect of stimulation × time), $p < 0.0001$.
(H) Stimulation of VMPO vGat-positive LepR neurons reduced T_{core} and T_{BAT}, but not T_{Tail}, in ChR2 mice at 10 Hz only (n = 5/group). Two-way ANOVA (effect of stimulation × time), $p < 0.0001$ for T_{core} and T_{BAT}.
The blue bar indicates light stimulation. Dunnett's test (for 10 Hz): *$p < 0.05$, **$p < 0.01$, ***$p < 0.001$, ****$p < 0.0001$. Data are mean ± SEM.

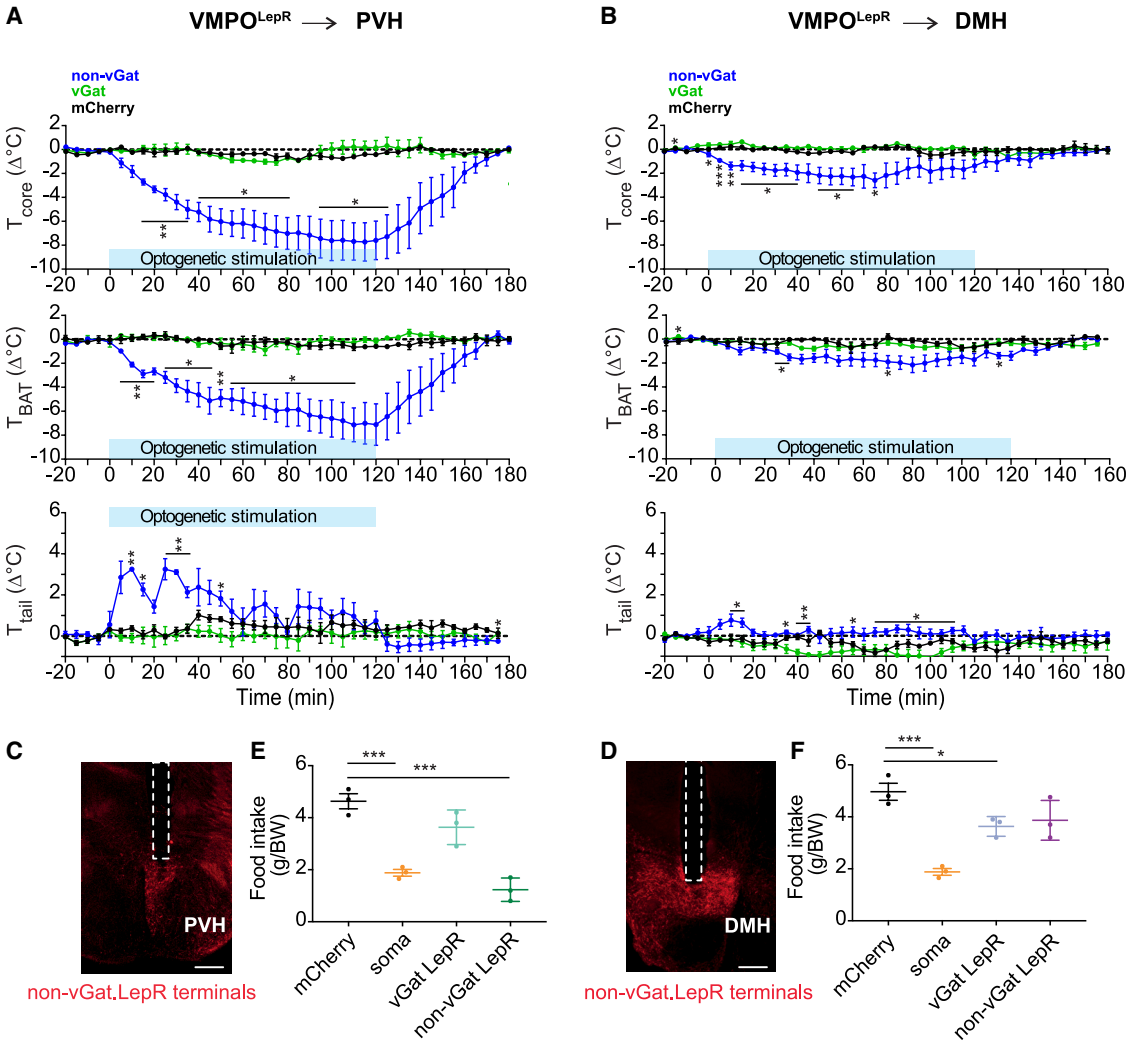

Figure 4. Predominantly VGAT-negative (excitatory) VMPO^{LepR}→PVH neuron projections inhibit thermogenesis and food intake

(A) Optogenetic stimulation (10 Hz) of non-vGat VMPO^{LepR}→PVH terminals (purple), but not vGat VMPO^{LepR} (green) or mCherry controls (black), reduced T_{core} and T_{BAT} and increased T_{Tail} (n = 3 per group).

(B) Optogenetic stimulation (10 Hz) of non-vGat VMPO^{LepR}→DMH terminals (purple), but not vGat VMPO^{LepR} terminals (green) or mCherry controls (black), produced a small but significant decrease in T_{core} and T_{BAT}, whereas T_{Tail} remained largely unchanged (n = 4 per group).

(A and B) Two-way ANOVA analysis with Fisher's LSD post hoc tests is reported.

(C and D) Representative histological images showing projections of vGat.LepR neurons (ChR2-mCherry, red) and optic fiber implantation sites (white dotted lines) in the PVH (C) and DMH (D). Scale bar, 200 μm.

(E and F) Food intake normalized to body weight during overnight optogenetic stimulation of VMPO^{LepR} somas or vGat VMPO^{LepR} and non-vGat-VMPO^{LepR} projections to the PVH (E) or DMH (F), as indicated. Cre-dependent mCherry expression in VMPO^{LepR} neurons with optic fibers targeting the PVH or DMH served as controls. Food intake was significantly reduced when vGat-negative (putatively excitatory) VMPO^{LepR} projections to the PVH were stimulated at 10 Hz. Vgat-positive projections terminating in the DMH also appeared to have a small but significant inhibitory effect on food intake. One-way ANOVA (n = 3 mice for each group).

*p < 0.05, **p < 0.01, ***p < 0.001, ****p < 0.0001.

Data in (A), (B), (E), and (F) are shown as mean ± SEM.

DISCUSSION

Several studies have implicated hypothalamic preoptic neurons in the suppression of energy expenditure and body temperature in mice, and activation of some of those neuronal populations also inhibits energy (food) intake.[13,30,32,41,47] At the extreme, activity of these neurons results in a long-lasting hypometabolic and hypothermic state,[48–51] similar to the state of torpor.[52] Therefore, these neurons have been dubbed *quiescence-inducing neurons* or, based on the diverse "marker" genes they express, QPLOT neurons (which stands for Qrfp, Ptger3, LepR, Opn5, and Tacr3 mRNA transcripts that these VMPO neurons co-express).[43]

However, the downstream neuronal pathways activated by these neurons are only incompletely understood.

Recently, it was shown that activation of excitatory (Vglut2-positive) rostral POA neurons that project to the PVH can inhibit food intake.[26] However, the authors of this study did not observe an effect on body/rectal temperature.

Please cite this article in press as: Bouaouda et al., Thermal-state-dependent control of body temperature and feeding by two intra-hypothalamic pathways, Current Biology (2026), https://doi.org/10.1016/j.cub.2026.01.074

CellPress
OPEN ACCESS

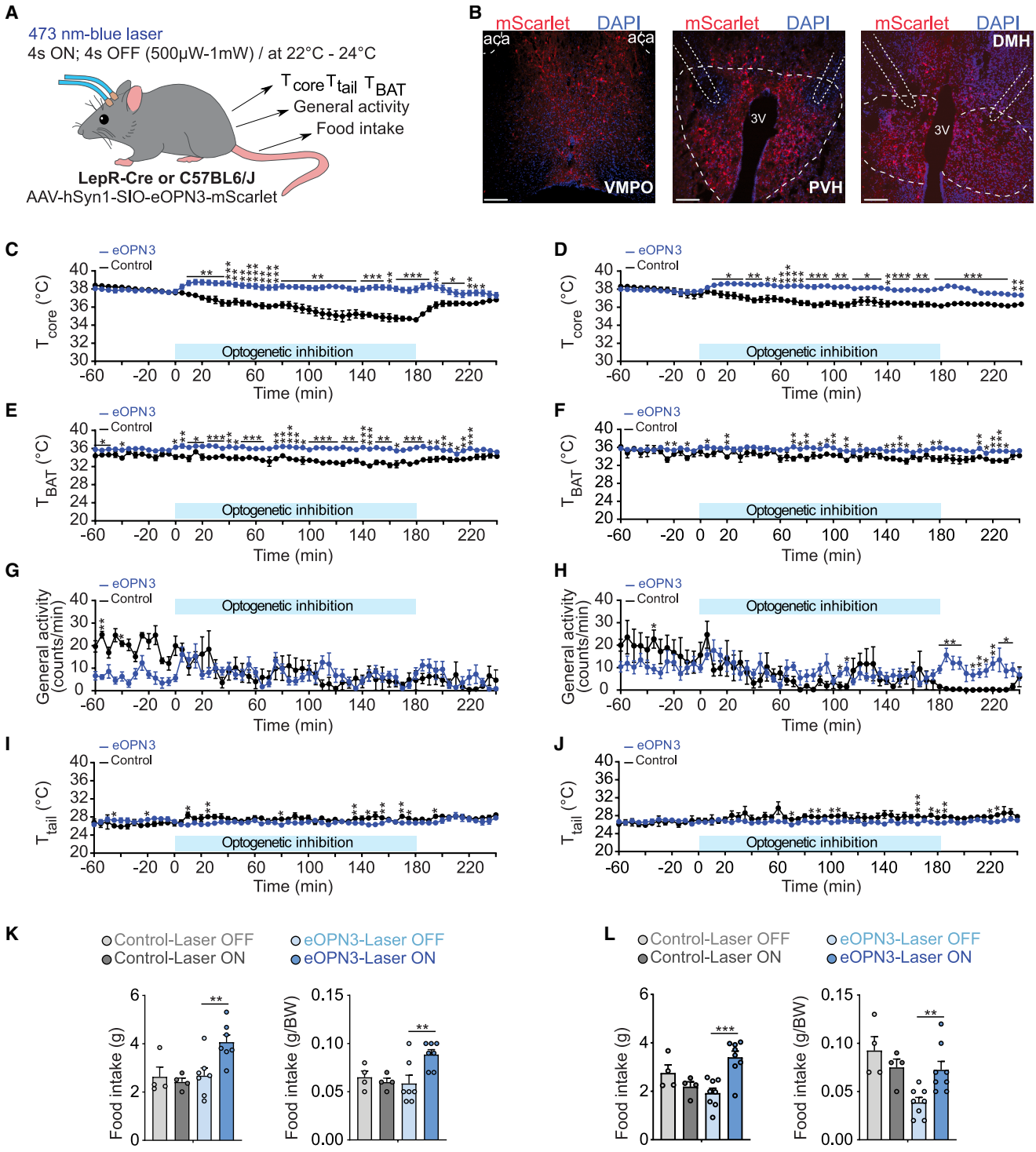

Figure 5. Optogenetic inhibition of VMPO^{LepR}→PVH and VMPO^{LepR}→DMH terminals at ≈23°C ambient temperature induces increases in body temperature and food intake

(A) Schematic of the optogenetic inhibition paradigm. Bilateral blue light illumination (473 nm, 500 µW–1 mW) was delivered in a 4-s ON/4-s OFF cycle for 3 h during the light phase or for 11 h during the dark phase (food intake experiments).

(B) Histological images showing eOPN3-mScarlet expression originating from LepR-positive VMPO projections innervating the PVH and DMH (white dotted outlines). Scale bars, 200 µm.

(C and D) Time course of core body temperature (Tcore) during 3 h of optogenetic inhibition (laser ON, blue bar) of VMPO^{LepR}→PVH (C, eOPN3 $n = 7$; controls $n = 4$) or VMPO^{LepR}→DMH (D, eOPN3 $n = 8$; controls $n = 4$) terminals.

(legend continued on next page)

Please cite this article in press as: Bouaouda et al., Thermal-state-dependent control of body temperature and feeding by two intra-hypothalamic pathways, Current Biology (2026), https://doi.org/10.1016/j.cub.2026.01.074

Using similar Vglut2-IRES-Cre mice, we found that indiscriminate stimulation of presumably heterogeneous VMPO^{Vglut2}→PVH terminals elicited several distinct behavioral and thermo-metabolic responses, resulting in no net effect on feeding but a small increase in T_{core}.

While this apparent discrepancy compared with our findings could in part reflect methodological differences (Qian et al. measured food intake in food-deprived mice during the day rather than at night and assessed body temperature using a rectal probe rather than by telemetric recording), it is likely that the complex and partially competing responses triggered by broad activation of excitatory pathways mask—or even negate—specific thermo-metabolic effects. This is perhaps best illustrated by the simultaneous activation of heat-gain (BAT thermogenesis) and heat-loss (tail vasodilation) responses upon stimulation of the VMPO^{Vglut2}→PVH pathway (Figures 2J, 2L, and S4K).

We cannot, however, rule out that in our optogenetic experiments activation of Vglut2-positive fibers "spilled over" into other pathways besides the PVH, thereby explaining some of the additional responses. Arguing against this possibility are previous findings demonstrating the involvement of PVH neurons in escape- or arousal-related behaviors.[53,54] Consistent with these reports, we observed robust agitation and increased activity upon optogenetic stimulation, which likely masked the food-intake measurements due to the strong behavioral activation of the animals.

By contrast, selective activation of the LepR/Vglut2 double-positive subpopulation produced more discrete responses: a reduction in both food intake and T_{core}, without detectable changes in locomotor activity. Importantly, performing the complementary experiment—optogenetic inhibition of the VMPO^{LepR}→PVH pathway using eOPN3—evoked the opposite effects, namely increased food intake and T_{core}.

Our study indicates that, alongside the established ARC to PVH pathway, there exists an additional pathway from the POA to PVH that decreases food intake and reduces body temperature. It will be important to determine whether distinct Vglut2-positive subtypes within the population of VMPO^{LepR}→PVH fibers selectively regulate feeding and specific thermoregulatory effectors such as BAT thermogenesis, vasomotion, heart rate, and others, or whether such functional specificity emerges downstream at the level of different PVH neuron populations that are innervated by VMPO^{LepR} fibers. The PVH contains different subpopulations of neurons that selectively modulate either food intake or energy expenditure.[10,24,33,55,56]

In this regard, it is interesting to note that a sympatho-inhibitory population has been postulated to reside in the PVH that, when activated, inhibits BAT thermogenesis.[23] This elusive group of PVH neurons has been further characterized to receive inhibitory input from rat insulin promotor (RIP)-Cre neurons in the ARC.[24] RIP neuron activity thereby increases BAT thermogenesis by inhibiting tonic activity of the PVH population. The origin of the tonic activity of these neurons is unknown, as is their molecular identity. We hypothesize that excitatory VMPO^{LepR} neurons contribute to the activity of these sympatho-inhibitory PVH neurons. We further speculate that VMPO^{LepR} neurons may also innervate MCR4-positive and/or prodynorphin (PDYN)-positive PVH neurons, both of which are known to suppress food intake.[22] Because inhibitory input from ARC neurons onto these PVH populations promotes feeding, it is consistent with our model that excitatory input from VMPO^{LepR} neurons onto the same PVH targets would instead reduce food intake. Although our intersectional strategy strongly suggests that a predominantly excitatory drive mediates this anorexigenic effect, it is important to note that the presence of Vglut2 expression, while generally indicative of an excitatory phenotype, may not in all cases fully capture the functional transmitter profile of VMPO^{LepR} projections, as recently highlighted.[38] In particular, components of GABAergic signaling may be present at projection terminals even when undetectable in neuronal somata, and hybrid neurons co-expressing glutamatergic and GABAergic markers have been reported. Ultimately, refined electrophysiological, pharmacologic, and genetic approaches will be required to determine the precise transmitter—or combination of transmitters—released from VMPO^{LepR} terminals in the PVH and DMH that give rise to the observed phenotypes.

Any PVH population that could mediate transient tail vasodilation is, to the best of our knowledge, currently unknown.

We observed varying magnitudes of body temperature responses, depending on whether we optogenetically stimulated fiber terminals versus neuron cell bodies (somas). We optogenetically stimulated the VMPO→PVH/DMH pathways unilaterally, and it is possible that stronger effects might have been observed with bilateral excitation, due to potential competitive interactions between the ipsilateral and contralateral PVH/DMH hemispheres and/or stronger overall pathway recruitment. Another potential explanation for this difference is that VMPO^{LepR} projections to PVH and DMH may interact synergistically so that the conjoint activation of both pathways together has the strongest effect. This interpretation is supported by our pathway-selective inhibition experiments: when inhibiting each pathway individually during heat exposure, we initially expected that blocking either projection might cause severe overheating. However, when only one pathway (for example, the DMH pathway) was inhibited, the other pathway (PVH) remained functional and could still partially mitigate overheating. This likely explains why the animals overheated but not to an extent that compromised their survival or health.

(E and F) Time course of BAT temperature (T_{BAT}) during 3 h of optogenetic inhibition of VMPO^{LepR}→PVH (E) or VMPO^{LepR}→DMH (F) terminals.
(G and H) Time course of general locomotor activity during optogenetic inhibition of VMPO^{LepR}→PVH (G) or VMPO^{LepR}→DMH (H) terminals.
(I and J) Time course of tail temperature (T_{Tail}) during optogenetic inhibition of VMPO^{LepR}→PVH (I) or VMPO^{LepR}→DMH (J) terminals.
(K and L) Overnight optogenetic inhibition (11 h, dark phase) of VMPO^{LepR}→PVH terminals (K) or VMPO^{LepR}→DMH terminals (L) at room temperature (22°C–24°C) increased food intake.
In (C)–(J), data are recorded every 5 min. Data in (C)–(L) are shown as mean ± SEM; repeated-measures two-way ANOVA with post hoc Fisher's LSD tests. Asterisks indicate statistically significant differences (*$p < 0.05$, **$p < 0.01$, ***$p < 0.001$).
See also Figures S5 and S6.

Please cite this article in press as: Bouaouda et al., Thermal-state-dependent control of body temperature and feeding by two intra-hypothalamic pathways, Current Biology (2026), https://doi.org/10.1016/j.cub.2026.01.074

CellPress
OPEN ACCESS

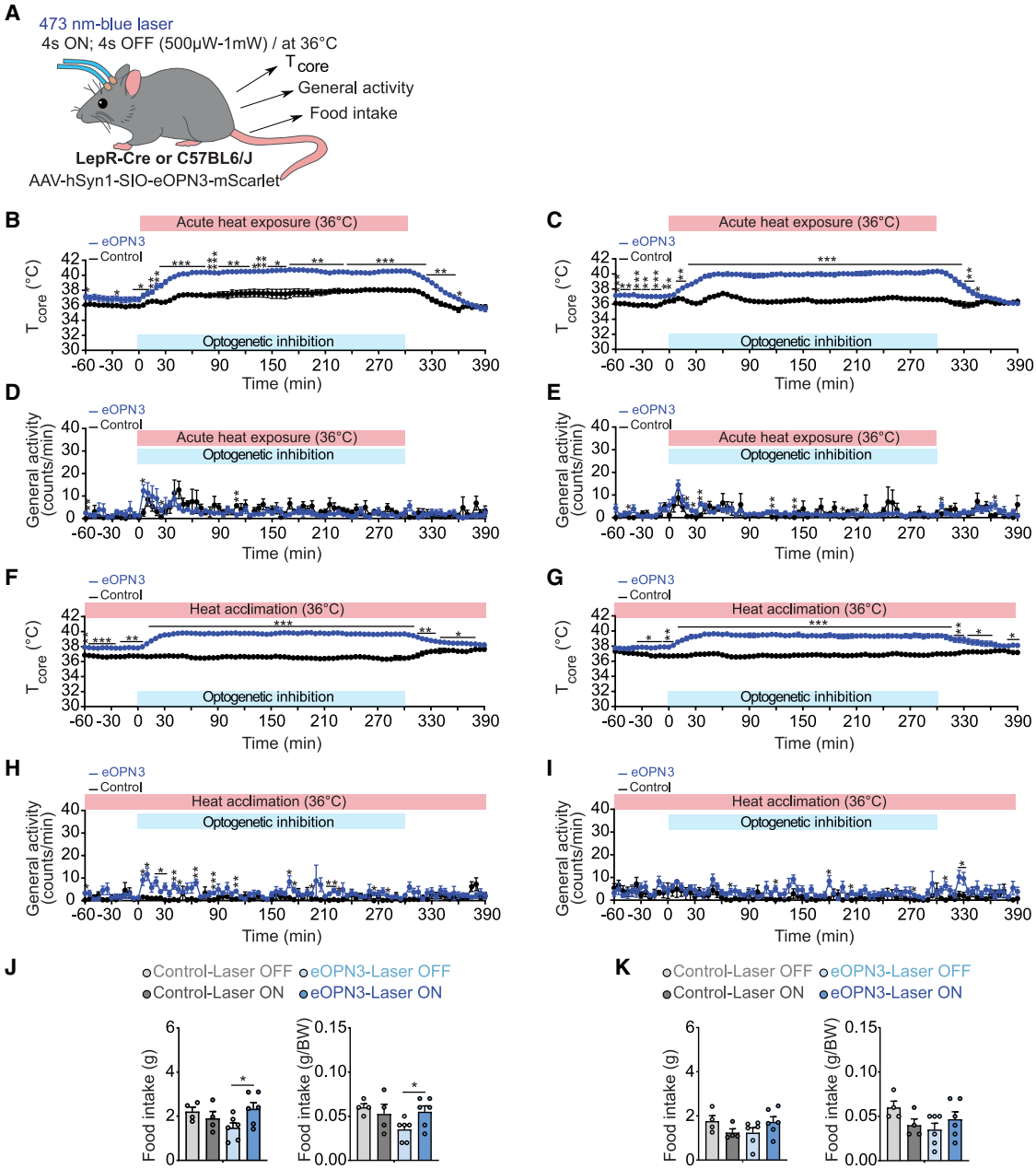

Figure 6. Optogenetic inhibition of VMPO^{LepR}→PVH and VMPO^{LepR}→DMH terminals at hot ambient temperature (36°C) induces robust hyperthermia and a modest increase in food intake via the VMPO^{LepR}→PVH pathway

(A) Schematic of the optogenetic inhibition paradigm. Bilateral blue light illumination (473 nm, 500 µW–1 mW) was delivered in a 4-s ON/4-s OFF cycle for 5 h during the light phase or for 11 h during the dark phase (food intake experiments).

(B and C) Time course of core body temperature (T_{core}) during acute heat exposure (36°C, 5 h) and optogenetic inhibition (laser ON, blue bar) of VMPO^{LepR}→PVH (B, eOPN3 $n = 6$; controls $n = 4$) or VMPO^{LepR}→DMH (C, eOPN3 $n = 8$; controls $n = 4$) terminals.

(D and E) Time course of general locomotor activity during acute heat exposure and optogenetic inhibition of VMPO^{LepR}→PVH (D) or VMPO^{LepR}→DMH (E) terminals.

(F and G) Time course of T_{core} during optogenetic inhibition (laser ON) for 5 h at 36°C of VMPO^{LepR}→PVH (F) or VMPO^{LepR}→DMH (G) terminals in mice previously heat acclimated (36°C for 4 weeks).

(H and I) Time course of general locomotor activity during optogenetic inhibition of VMPO^{LepR}→PVH (H) or VMPO^{LepR}→DMH (I) terminals in mice previously exposed to long-term heat acclimation (36°C for 4 weeks).

(J and K) Overnight optogenetic inhibition (11 h, dark phase) of VMPOLepR→PVH (J) or VMPO^{LepR}→DMH (K) terminals at 36°C in heat-acclimated mice. Inhibition of the VMPO^{LepR}→PVH pathway increased food intake, whereas inhibition of the VMPO^{LepR}→DMH pathway had no significant effect.

In (B)–(I), data were recorded every 5 min. Data in (B)–(K) are shown as mean ± SEM; repeated-measures two-way ANOVA with post hoc Fisher's LSD tests. Asterisks indicate statistically significant differences (*$p < 0.05$, **$p < 0.01$, ***$p < 0.001$).

See also Figure S7.

Please cite this article in press as: Bouaouda et al., Thermal-state-dependent control of body temperature and feeding by two intra-hypothalamic pathways, Current Biology (2026), https://doi.org/10.1016/j.cub.2026.01.074

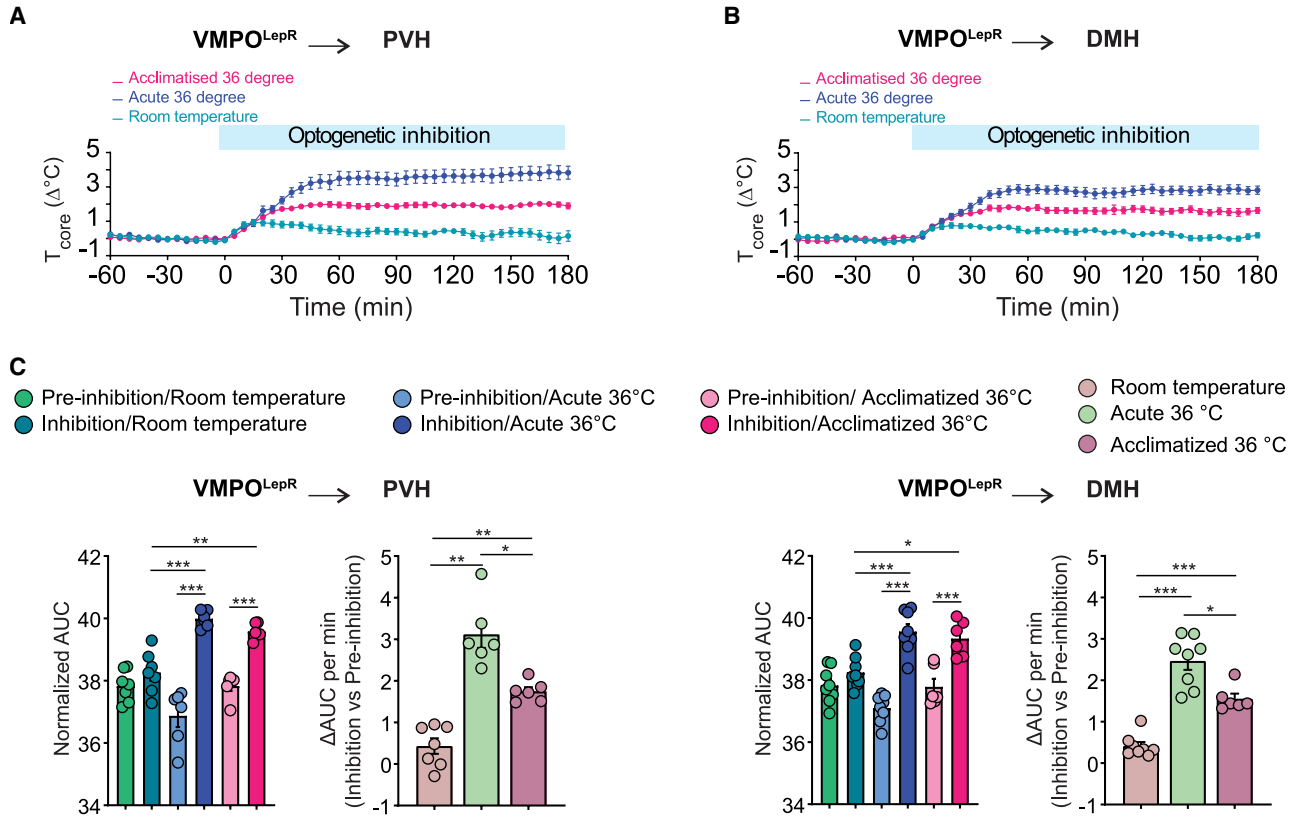

Figure 7. Optogenetic inhibition of VMPOLepR→PVH and VMPOLepR→DMH terminals induces robust hyperthermia under hot, but not cool, ambient temperatures

(A and B) Time course of core body temperature (T_{core}) in LepR-Cre mice at room temperature (22°C–24°C; turquoise), during acute heat exposure (36°C; purple), or following long-term heat acclimation (36°C for 4 weeks; magenta), recorded during optogenetic inhibition of VMPO^{LepR}→PVH (A) or VMPO^{LepR}→DMH (B) terminals. Traces are derived from eOPN3-expressing animals shown in Figures 5 and 6.

(C) Normalized area under the curve (AUC) of T_{core} before ("pre-inhibition" = laser OFF) and during optogenetic inhibition ("inhibition" = laser ON) of VMPO^{lepR}→PVH and VMPO^{lepR}→DMH terminals. ΔAUC analysis (laser OFF versus laser ON) shows that inhibition of either pathway induces robust hyperthermia during acute and long-term heat exposure (36°C) but not at 22°C–24°C ambient temperature.

In (A) and (B), data are shown as mean ± SEM (see Figures 5 and 6). In (C), two-way ANOVA analysis with Tukey's post hoc comparisons was performed. Asterisks indicate statistical significance (*$p < 0.05$, **$p < 0.01$, ***$p < 0.001$)

Of note, stimulation of non-vGat.LepR VMPO cell bodies produced more pronounced tail vasodilation (Figure 3G) than stimulation of non-vGat.LepR VMPO fibers projecting to the PVH (Figure 4A). This makes it plausible that VMPO^{LepR} neurons modulate body temperature via additional, yet unrecognized pathways, and that our initial anterograde labeling may have missed sparse or diffuse projections to other regions. In the context of vasodilation, the RP is a well-established obligatory output center.[16] Additionally, it is possible that VMPO^{LepR} pathways modulate other physiological functions influencing body temperature—such as heart rate—which we did not measure here. Future work will be required to determine whether VMPO^{LepR} neurons engage the RP—either monosynaptically or polysynaptically—or whether other CNS sites relevant for thermo-metabolic regulation are involved.

Considering potential physiological rationales of this bifunctional pathway raises intriguing questions: at first glance, inhibiting energy expenditure and food intake simultaneously may seem counterintuitive: when energy is low, there should be a strong drive to take up more energetic fuel/food. An important question is under which physiological conditions—outside of the extreme case of torpor—hypometabolism and body cooling are simultaneously engaged and when the VMPO^{LepR} neuronal network is recruited.

Exposure to a warm or hot environment for an extended period is known to inhibit food intake, suppress energy expenditure, and recruit heat-loss responses.[3,57,58] Together, these adaptations prevent overheating and resemble the physiological state observed when the VMPO^{LepR}→PVH/DMH circuits are activated.

Intriguingly, VMPO^{LepR} neurons have been shown to respond to peripheral warmth and heat stimuli.[13] Moreover, we recently discovered that VMPO^{LepR} neurons undergo a plastic transformation to become tonically active, warm-sensitive neurons when animals are exposed to elevated temperatures for prolonged periods. This increased excitability of VMPO^{LepR} neurons is crucial for enhancing the animals' heat tolerance.[31]

In agreement with these previous findings, we now show that the contribution of the VMPO^{LepR}→PVH/DMH pathways to body

Please cite this article in press as: Bouaouda et al., Thermal-state-dependent control of body temperature and feeding by two intra-hypothalamic pathways, Current Biology (2026), https://doi.org/10.1016/j.cub.2026.01.074

temperature regulation is amplified under hot environmental conditions: inhibiting either pathway increases body temperature much more robustly at high ambient temperatures compared with cooler conditions (22°C–24°C) (Figure 7). This temperature-dependent difference may even be underestimated, as at room temperature control animals exhibit a subtle decrease in T_{core} (Figures 5C and 5D), likely reflecting light-induced warming of the hypothalamus that engages homeostatic cooling responses—a phenomenon long appreciated in principle and recently demonstrated using optic-fiber-based illumination of the POA.[59]

It is possible that simultaneous inhibition of both pathways (rather than separately, as done in this study) would have an even stronger effect on body temperature and might render animals incapable of tolerating heat. Based on our pathway stimulation experiments, which demonstrated PVH-mediated cutaneous tail vasodilation, inhibition of the same pathway would be expected to reduce heat dissipation and thereby exacerbate hyperthermia. However, because we did not directly measure tail vasomotor responses during eOPN3-mediated inhibition under warm or hot environmental conditions, this interpretation remains speculative, and it is currently unclear to what extent PVH pathway inhibition counteracts warming-induced tail vasodilation. In addition, we noted that pathway inhibition induced a stronger hyperthermic response during acute heat exposure than at the end of heat acclimation (Figure 7). Because modulation of BAT activity contributes —at least in part— to changes in T_{core}, a likely explanation for the reduced effect after heat acclimation is the well-described atrophy and functional downregulation of BAT under prolonged heat exposure, which would limit its capacity to contribute to hyperthermia upon eOPN3-mediated pathway inhibition.

Interestingly, the thermal-state dependence of feeding regulation differed from that of body temperature. While the $VMPO^{LepR}$→PVH pathway—but not the $VMPO^{LepR}$→DMH pathway—significantly contributed to food-intake inhibition under hot conditions, the influence of either pathway on feeding appeared more pronounced under cooler (room temperature) conditions. Given that the VMPO neurons we studied here are primarily marked by the leptin receptor, it is possible that leptin mediates this thermal-state-dependent switch. $VMPO^{LepR}$ neuron activity can be modulated by leptin.[60] Interestingly, Yu et al. find that *in vivo* leptin application into the POA/VMPO appears to influence energy expenditure mostly (or exclusively) when the animals are fasted.[60] Thus, leptin's capacity to exert regulatory control over these neurons may be state-dependent and potentially maximal under conditions such as fasting. Whether the thermal state (thermal exposure) can alter the modulatory capacity and/or sensitivity of leptin on $VMPO^{LepR}$ neurons is, to the best of our knowledge, currently unknown.

In summary, and in the context of previous findings, we propose that—beyond their role in torpor induction—a primary function of $VMPO^{LepR}$ (QPLOT) neurons is to fine-tune thermometabolic pathways during heat exposure, thereby enabling animals to adapt and survive in warm environments.

Future work will have to uncover the physiological relevance and downstream pathways of $VMPO^{LepR}$ neurons not only in mice but also across other animal species, including humans.

RESOURCE AVAILABILITY

Lead contact

Requests for further information and resources should be directed to and will be fulfilled by the lead contact, Jan Siemens (jan.siemens@pharma.uni-heidelberg.de).

Materials availability

This study did not generate any new, unique reagents.

Data and code availability

- The data associated with the figures are provided as source data files, with all data included in subfolders named correspondingly to the figures, via the HeiData server of Heidelberg University at https://doi.org/10.11588/DATA/YUPKKD.
- This study did not generate any unique datasets or code.

ACKNOWLEDGMENTS

We thank Amandine Cavaroc, Christine Siegmund, and Lisa Vierbaum for technical support; Henning Fenselau and Katrin Schrenk-Siemens for inspiring discussions and critical reading of the manuscript; Anke Tappe-Theodor for her help with corticosterone measurements; and the Nikon Imaging Center at Heidelberg University for support with confocal microscopy. Funding: the authors gratefully acknowledge the data storage service SDS@hd supported by the Ministry of Science, Research, and the Arts, Baden-Württemberg (MWK) and the German Research Foundation (DFG) through grants INST 35/1803-1 FUGG and INST 35/1804-1 LAGG. This work was supported by the European Research Council ERC-CoG-772395, the German Research Foundation SFB/TRR 152 (to J.S.), and the European Molecular Biology Organization (EMBO) postdoctoral fellowship (to S.N.).

AUTHOR CONTRIBUTIONS

J.S., together with H.B. and S.N., conceived the project. H.B. and S.N. performed all experiments.

DECLARATION OF INTERESTS

The authors declare no competing interests.

DECLARATION OF GENERATIVE AI AND AI-ASSISTED TECHNOLOGIES IN THE WRITING PROCESS

During the preparation of this work, the authors used ChatGPT 5.2 to assist with correcting spelling and grammar in some sections of the manuscript. After using this tool/service, the authors reviewed and edited all content as needed and take full responsibility for the final version of the published article.

STAR★METHODS

Detailed methods are provided in the online version of this paper and include the following:

- KEY RESOURCES TABLE
- EXPERIMENTAL MODEL AND STUDY PARTICIPANT DETAILS
  - Transgenic mouse lines
  - Mouse husbandry
  - Viral AAV constructs
- METHOD DETAILS
  - Virus injection and optic fiber implantation
  - Optogenetic experiments
  - Locomotor activity and temperature recordings
  - Food intake assay
  - Fecal corticosterone metabolite measurements
  - Electrophysiological recordings
  - Immunohistochemistry
  - Retrograde labelling of LepR neurons

- QUANTIFICATION AND STATISTICAL ANALYSIS

SUPPLEMENTAL INFORMATION

Supplemental information can be found online at https://doi.org/10.1016/j.cub.2026.01.074.

Received: April 19, 2024
Revised: December 4, 2025
Accepted: January 30, 2026

REFERENCES

1. Nedergaard, J., and Cannon, B. (2018). Brown adipose tissue as a heat-producing thermoeffector. Handb. Clin. Neurol. *156*, 137–152. https://doi.org/10.1016/B978-0-444-63912-7.00009-6.
2. Romanovsky, A.A. (2018). The thermoregulation system and how it works. Handb. Clin. Neurol. *156*, 3–43. https://doi.org/10.1016/B978-0-444-63912-7.00001-1.
3. Gordon, C.J. (1993). Temperature Regulation in Laboratory Rodents (Cambridge University Press). https://doi.org/10.1017/CBO9780511565595.
4. Hacker, J.B., and Ternouth, J.H.; Australian Society of Animal Production, and International Symposium on the Nutrition of Herbivores (1987). The Nutrition of Herbivores (Academic Press).
5. Marriott, B.M.; Institute of Medicine (US) Committee on Military Nutrition Research (1993). Nutritional Needs in Hot Environments: Applications for Military Personnel in Field Operations (National Academy Press).
6. Horvath, T.L., Stachenfeld, N.S., and Diano, S. (2014). A temperature hypothesis of hypothalamus-driven obesity. Yale J. Biol. Med. *87*, 149–158.
7. Morrison, S.F., and Nakamura, K. (2019). Central Mechanisms for Thermoregulation. Annu. Rev. Physiol. *81*, 285–308. https://doi.org/10.1146/annurev-physiol-020518-114546.
8. Morrison, S.F., Nakamura, K., and Madden, C.J. (2008). Central control of thermogenesis in mammals. Exp. Physiol. *93*, 773–797. https://doi.org/10.1113/expphysiol.2007.041848.
9. Tran, L.T., Park, S., Kim, S.K., Lee, J.S., Kim, K.W., and Kwon, O. (2022). Hypothalamic control of energy expenditure and thermogenesis. Exp. Mol. Med. *54*, 358–369. https://doi.org/10.1038/s12276-022-00741-z.
10. An, J.J., Liao, G.Y., Kinney, C.E., Sahibzada, N., and Xu, B. (2015). Discrete BDNF Neurons in the Paraventricular Hypothalamus Control Feeding and Energy Expenditure. Cell Metab. *22*, 175–188. https://doi.org/10.1016/j.cmet.2015.05.008.
11. Houtz, J., Liao, G.Y., An, J.J., and Xu, B. (2021). Discrete TrkB-expressing neurons of the dorsomedial hypothalamus regulate feeding and thermogenesis. Proc. Natl. Acad. Sci. USA *118*, e2017218118. https://doi.org/10.1073/pnas.2017218118.
12. Schneeberger, M., Parolari, L., Das Banerjee, T., Bhave, V., Wang, P., Patel, B., Topilko, T., Wu, Z., Choi, C.H.J., Yu, X., et al. (2019). Regulation of Energy Expenditure by Brainstem GABA Neurons. Cell *178*, 672–685.e12. https://doi.org/10.1016/j.cell.2019.05.048.
13. Yu, S., Qualls-Creekmore, E., Rezai-Zadeh, K., Jiang, Y., Berthoud, H.R., Morrison, C.D., Derbenev, A.V., Zsombok, A., and Münzberg, H. (2016). Glutamatergic Preoptic Area Neurons That Express Leptin Receptors Drive Temperature-Dependent Body Weight Homeostasis. J. Neurosci. *36*, 5034–5046. https://doi.org/10.1523/JNEUROSCI.0213-16.2016.
14. Siemens, J., and Kamm, G.B. (2018). Cellular populations and thermosensing mechanisms of the hypothalamic thermoregulatory center. Pflugers Arch. *470*, 809–822. https://doi.org/10.1007/s00424-017-2101-0.
15. Tan, C.L., and Knight, Z.A. (2018). Regulation of Body Temperature by the Nervous System. Neuron *98*, 31–48. https://doi.org/10.1016/j.neuron.2018.02.022.
16. Madden, C.J., and Morrison, S.F. (2019). Central nervous system circuits that control body temperature. Neurosci. Lett. *696*, 225–232. https://doi.org/10.1016/j.neulet.2018.11.027.
17. Jais, A., and Brüning, J.C. (2022). Arcuate Nucleus-Dependent Regulation of Metabolism-Pathways to Obesity and Diabetes Mellitus. Endocr. Rev. *43*, 314–328. https://doi.org/10.1210/endrev/bnab025.
18. Brüning, J.C., and Fenselau, H. (2023). Integrative neurocircuits that control metabolism and food intake. Science *381*, eabl7398. https://doi.org/10.1126/science.abl7398.
19. Atasoy, D., Betley, J.N., Su, H.H., and Sternson, S.M. (2012). Deconstruction of a neural circuit for hunger. Nature *488*, 172–177. https://doi.org/10.1038/nature11270.
20. Fenselau, H., Campbell, J.N., Verstegen, A.M.J., Madara, J.C., Xu, J., Shah, B.P., Resch, J.M., Yang, Z., Mandelblat-Cerf, Y., Livneh, Y., and Lowell, B.B. (2017). A rapidly acting glutamatergic ARC→PVH satiety circuit postsynaptically regulated by α-MSH. Nat. Neurosci. *20*, 42–51. https://doi.org/10.1038/nn.4442.
21. Garfield, A.S., Li, C., Madara, J.C., Shah, B.P., Webber, E., Steger, J.S., Campbell, J.N., Gavrilova, O., Lee, C.E., Olson, D.P., et al. (2015). A neural basis for melanocortin-4 receptor-regulated appetite. Nat. Neurosci. *18*, 863–871. https://doi.org/10.1038/nn.4011.
22. Li, M.M., Madara, J.C., Steger, J.S., Krashes, M.J., Balthasar, N., Campbell, J.N., Resch, J.M., Conley, N.J., Garfield, A.S., and Lowell, B.B. (2019). The Paraventricular Hypothalamus Regulates Satiety and Prevents Obesity via Two Genetically Distinct Circuits. Neuron *102*, 653–667.e6. https://doi.org/10.1016/j.neuron.2019.02.028.
23. Madden, C.J., and Morrison, S.F. (2009). Neurons in the paraventricular nucleus of the hypothalamus inhibit sympathetic outflow to brown adipose tissue. Am. J. Physiol. Regul. Integr. Comp. Physiol. *296*, R831–R843. https://doi.org/10.1152/ajpregu.91007.2008.
24. Kong, D., Tong, Q., Ye, C., Koda, S., Fuller, P.M., Krashes, M.J., Vong, L., Ray, R.S., Olson, D.P., and Lowell, B.B. (2012). GABAergic RIP-Cre neurons in the arcuate nucleus selectively regulate energy expenditure. Cell *151*, 645–657. https://doi.org/10.1016/j.cell.2012.09.020.
25. Piñol, R.A., Mogul, A.S., Hadley, C.K., Saha, A., Li, C., Škop, V., Province, H.S., Xiao, C., Gavrilova, O., Krashes, M.J., and Reitman, M.L. (2021). Preoptic BRS3 neurons increase body temperature and heart rate via multiple pathways. Cell Metab. *33*, 1389–1403.e6. https://doi.org/10.1016/j.cmet.2021.05.001.
26. Qian, S., Yan, S., Pang, R., Zhang, J., Liu, K., Shi, Z., Wang, Z., Chen, P., Zhang, Y., Luo, T., et al. (2022). A temperature-regulated circuit for feeding behavior. Nat. Commun. *13*, 4229. https://doi.org/10.1038/s41467-022-31917-w.
27. Suwannapaporn, P., Chaiyabutr, N., Wanasuntronwong, A., and Thammacharoen, S. (2022). Arcuate proopiomelanocortin is part of a novel neural connection for short-term low-degree of high ambient temperature effects on food intake. Physiol. Behav. *245*, 113687. https://doi.org/10.1016/j.physbeh.2021.113687.
28. Friedman, J.M. (2019). Leptin and the endocrine control of energy balance. Nat. Metab. *1*, 754–764. https://doi.org/10.1038/s42255-019-0095-y.
29. Fischer, A.W., Hoefig, C.S., Abreu-Vieira, G., de Jong, J.M.A., Petrovic, N., Mittag, J., Cannon, B., and Nedergaard, J. (2016). Leptin Raises Defended Body Temperature without Activating Thermogenesis. Cell Rep. *14*, 1621–1631. https://doi.org/10.1016/j.celrep.2016.01.041.
30. Machado, N.L.S., and Saper, C.B. (2022). Genetic identification of preoptic neurons that regulate body temperature in mice. Temperature (Austin) *9*, 14–22. https://doi.org/10.1080/23328940.2021.1993734.
31. Ambroziak, W., Nencini, S., Pohle, J., Zuza, K., Pino, G., Lundh, S., Araujo-Sousa, C., Goetz, L.I.L., Schrenk-Siemens, K., Manoj, G., et al. (2025). Thermally induced neuronal plasticity in the hypothalamus mediates heat tolerance. Nat. Neurosci. *28*, 346–360. https://doi.org/10.1038/s41593-024-01830-0.
32. Tan, C.L., Cooke, E.K., Leib, D.E., Lin, Y.C., Daly, G.E., Zimmerman, C.A., and Knight, Z.A. (2016). Warm-Sensitive Neurons that Control Body

Temperature. Cell *167*, 47–59.e15. https://doi.org/10.1016/j.cell.2016.08.028.

33. Andermann, M.L., and Lowell, B.B. (2017). Toward a Wiring Diagram Understanding of Appetite Control. Neuron *95*, 757–778. https://doi.org/10.1016/j.neuron.2017.06.014.
34. Hao, S., Yang, H., Wang, X., He, Y., Xu, H., Wu, X., Pan, L., Liu, Y., Lou, H., Xu, H., et al. (2019). The Lateral Hypothalamic and BNST GABAergic Projections to the Anterior Ventrolateral Periaqueductal Gray Regulate Feeding. Cell Rep. *28*, 616–624.e5. https://doi.org/10.1016/j.celrep.2019.06.051.
35. Imoto, D., Yamamoto, I., Matsunaga, H., Yonekura, T., Lee, M.L., Kato, K.X., Yamasaki, T., Xu, S., Ishimoto, T., Yamagata, S., et al. (2021). Refeeding activates neurons in the dorsomedial hypothalamus to inhibit food intake and promote positive valence. Mol. Metab. *54*, 101366. https://doi.org/10.1016/j.molmet.2021.101366.
36. Morrison, S.F., and Nakamura, K. (2011). Central neural pathways for thermoregulation. Front. Biosci. (Landmark Ed.) *16*, 74–104. https://doi.org/10.2741/3677.
37. Morrison, S.F., Nakamura, K., and Tupone, D. (2022). Thermoregulation in mice: The road to understanding torpor hypothermia and the shortcomings of a circuit for generating fever. Temperature (Austin) *9*, 8–11. https://doi.org/10.1080/23328940.2021.2021059.
38. Nakamura, Y., Yahiro, T., Fukushima, A., Kataoka, N., Hioki, H., and Nakamura, K. (2022). Prostaglandin EP3 receptor-expressing preoptic neurons bidirectionally control body temperature via tonic GABAergic signaling. Sci. Adv. *8*, eadd5463. https://doi.org/10.1126/sciadv.add5463.
39. Abbott, S.B.G., and Saper, C.B. (2017). Median preoptic glutamatergic neurons promote thermoregulatory heat loss and water consumption in mice. J. Physiol. *595*, 6569–6583. https://doi.org/10.1113/JP274667.
40. Aten, S., Lynch, N., Saper, C.B., and Machado, N.L.S. (2025). A brain-body perspective on thermoregulatory adaptation. Curr. Biol. *35*, R1016–R1028. https://doi.org/10.1016/j.cub.2025.09.023.
41. Song, K., Wang, H., Kamm, G.B., Pohle, J., Reis, F.C., Heppenstall, P., Wende, H., and Siemens, J. (2016). The TRPM2 channel is a hypothalamic heat sensor that limits fever and can drive hypothermia. Science *353*, 1393–1398. https://doi.org/10.1126/science.aaf7537.
42. Kroeger, D., Absi, G., Gagliardi, C., Bandaru, S.S., Madara, J.C., Ferrari, L.L., Arrigoni, E., Münzberg, H., Scammell, T.E., Saper, C.B., and Vetrivelan, R. (2018). Galanin neurons in the ventrolateral preoptic area promote sleep and heat loss in mice. Nat. Commun. *9*, 4129. https://doi.org/10.1038/s41467-018-06590-7.
43. Upton, B.A., D'Souza, S.P., and Lang, R.A. (2021). QPLOT Neurons-Converging on a Thermoregulatory Preoptic Neuronal Population. Front. Neurosci. *15*, 665762. https://doi.org/10.3389/fnins.2021.665762.
44. Douglass, A.M., Resch, J.M., Madara, J.C., Kucukdereli, H., Yizhar, O., Grama, A., Yamagata, M., Yang, Z., and Lowell, B.B. (2023). Neural basis for fasting activation of the hypothalamic-pituitary-adrenal axis. Nature *620*, 154–162. https://doi.org/10.1038/s41586-023-06358-0.
45. He, X.J., and Banghart, M.R. (2021). It's lights out for presynaptic terminals. Neuron *109*, 1755–1757. https://doi.org/10.1016/j.neuron.2021.05.015.
46. Mahn, M., Saraf-Sinik, I., Patil, P., Pulin, M., Bitton, E., Karalis, N., Bruentgens, F., Palgi, S., Gat, A., Dine, J., et al. (2021). Efficient optogenetic silencing of neurotransmitter release with a mosquito rhodopsin. Neuron *109*, 1621–1635.e8. https://doi.org/10.1016/j.neuron.2021.03.013.
47. Zhang, K.X., D'Souza, S., Upton, B.A., Kernodle, S., Vemaraju, S., Nayak, G., Gaitonde, K.D., Holt, A.L., Linne, C.D., Smith, A.N., et al. (2020). Violet-light suppression of thermogenesis by opsin 5 hypothalamic neurons. Nature *585*, 420–425. https://doi.org/10.1038/s41586-020-2683-0.
48. Hrvatin, S., Sun, S., Wilcox, O.F., Yao, H., Lavin-Peter, A.J., Cicconet, M., Assad, E.G., Palmer, M.E., Aronson, S., Banks, A.S., et al. (2020). Neurons that regulate mouse torpor. Nature *583*, 115–121. https://doi.org/10.1038/s41586-020-2387-5.
49. Takahashi, T.M., Sunagawa, G.A., Soya, S., Abe, M., Sakurai, K., Ishikawa, K., Yanagisawa, M., Hama, H., Hasegawa, E., Miyawaki, A., et al. (2020). A discrete neuronal circuit induces a hibernation-like state in rodents. Nature *583*, 109–114. https://doi.org/10.1038/s41586-020-2163-6.
50. Zhang, Z., Reis, F.M.C.V., He, Y., Park, J.W., DiVittorio, J.R., Sivakumar, N., van Veen, J.E., Maesta-Pereira, S., Shum, M., Nichols, I., et al. (2020). Estrogen-sensitive medial preoptic area neurons coordinate torpor in mice. Nat. Commun. *11*, 6378. https://doi.org/10.1038/s41467-020-20050-1.
51. Machado, N.L.S., Lynch, N., Costa, L.H.A., Melville, D., Kucukdereli, H., Kaur, S., Banks, A.S., Raffin, F., Ramirez-Plascencia, O.D., Aten, S., et al. (2025). Preoptic EP3R neurons constitute a two-way switch for fever and torpor. Nature *644*, 463–472. https://doi.org/10.1038/s41586-025-09056-1.
52. Swoap, S.J. (2008). The pharmacology and molecular mechanisms underlying temperature regulation and torpor. Biochem. Pharmacol. *76*, 817–824. https://doi.org/10.1016/j.bcp.2008.06.017.
53. Wang, F., Chen, Y., Lin, Y., Wang, X., Li, K., Han, Y., Wu, J., Shi, X., Zhu, Z., Long, C., et al. (2023). A parabrachial to hypothalamic pathway mediates defensive behavior. eLife *12*, e85450. https://doi.org/10.7554/eLife.85450.
54. Daviu, N., Füzesi, T., Rosenegger, D.G., Rasiah, N.P., Sterley, T.L., Peringod, G., and Bains, J.S. (2020). Paraventricular nucleus CRH neurons encode stress controllability and regulate defensive behavior selection. Nat. Neurosci. *23*, 398–410. https://doi.org/10.1038/s41593-020-0591-0.
55. Krashes, M.J., Shah, B.P., Madara, J.C., Olson, D.P., Strochlic, D.E., Garfield, A.S., Vong, L., Pei, H., Watabe-Uchida, M., Uchida, N., et al. (2014). An excitatory paraventricular nucleus to AgRP neuron circuit that drives hunger. Nature *507*, 238–242. https://doi.org/10.1038/nature12956.
56. Sutton, A.K., Pei, H., Burnett, K.H., Myers, M.G., Jr., Rhodes, C.J., and Olson, D.P. (2014). Control of food intake and energy expenditure by Nos1 neurons of the paraventricular hypothalamus. J. Neurosci. *34*, 15306–15318. https://doi.org/10.1523/JNEUROSCI.0226-14.2014.
57. Taylor, N.A.S. (2014). Human heat adaptation. Compr. Physiol. *4*, 325–365. https://doi.org/10.1002/cphy.c130022.
58. Zakrzewski-Fruer, J.K., Horsfall, R.N., Cottrill, D., and Hough, J. (2021). Acute exposure to a hot ambient temperature reduces energy intake but does not affect gut hormones in men during rest. Br. J. Nutr. *125*, 951–959. https://doi.org/10.1017/S0007114520002792.
59. Zhou, Q., Fu, X., Xu, J., Dong, S., Liu, C., Cheng, D., Gao, C., Huang, M., Liu, Z., Ni, X., et al. (2023). Hypothalamic warm-sensitive neurons require TRPC4 channel for detecting internal warmth and regulating body temperature in mice. Neuron *111*, 387–404.e8. https://doi.org/10.1016/j.neuron.2022.11.008.
60. Yu, S., Cheng, H., François, M., Qualls-Creekmore, E., Huesing, C., He, Y., Jiang, Y., Gao, H., Xu, Y., Zsombok, A., et al. (2018). Preoptic leptin signaling modulates energy balance independent of body temperature regulation. eLife *7*, e33505. https://doi.org/10.7554/eLife.33505.
61. Touma, C., Sachser, N., Möstl, E., and Palme, R. (2003). Effects of sex and time of day on metabolism and excretion of corticosterone in urine and feces of mice. Gen. Comp. Endocrinol. *130*, 267–278. https://doi.org/10.1016/s0016-6480(02)00620-2.
62. Segelcke, D., Talbot, S.R., Palme, R., La Porta, C., Pogatzki-Zahn, E., Bleich, A., and Tappe-Theodor, A. (2023). Experimenter familiarization is a crucial prerequisite for assessing behavioral outcomes and reduces stress in mice not only under chronic pain conditions. Sci. Rep. *13*, 2289. https://doi.org/10.1038/s41598-023-29052-7.

Please cite this article in press as: Bouaouda et al., Thermal-state-dependent control of body temperature and feeding by two intra-hypothalamic pathways, Current Biology (2026), https://doi.org/10.1016/j.cub.2026.01.074

STAR★METHODS

KEY RESOURCES TABLE

REAGENT or RESOURCE	SOURCE	IDENTIFIER
Antibodies		
Chicken polyclonal anti-GFP	Rockland	Cat# 600-901-215
Rabbit polyclonal anti-mCherry	ThermoFisher	Cat# PA5-34974; PRID: AB_2552323
Rabbit polyclonal anti DsRed	Takara Bio	Cat# 632496
Goat anti-Chicken IgY (H+L) Secondary Antibody, Alexa Fluor™ 488	Invitrogen	Cat# A-11039; PRID: AB_2534096
F(ab')2-Goat anti-Rabbit IgG (H+L) Cross-Adsorbed Secondary Antibody, Alexa Fluor™ 555	Invitrogen	Cat# A-21430; PRID: AB_2535851
Bacterial and virus strains		
ssAAV-DJ/2-hSyn1-chI-dlox-ChR2(H134R)_mCherry(rev)-dlox-WPRE-hGHp(A)	Zurich Viral Core	v332-DJ
ssAAV-DJ/2-hEF1α-dlox-ChR2(H134R)_EYFP(rev)-dlox-WPRE-hGHp(A)	Zurich Viral Core	v214-DJ
ssAAV-DJ/2-hSyn1-chI-dlox-mCherry(rev)-dlox-WPRE-hGHp(A)	Zurich Viral Core	v385-DJ
ssAAV-retro/2-shortCAG-dlox-EGFP(rev)-dlox-WPRE-SV40p(A)	Zurich Viral Core	v158-retro
ssAAV-retro/2-CAG-dlox-tdTomato(rev)-dlox-WPRE-bGHp(A)	Zurich Viral Core	v167-retro
ssAAV DJ/2-hSyn1-chI-Con/Fon(ChR2 (H134R)_EYFP)-WPRE-hGHp(A)	Zurich Viral Core	v333-DJ
ssAAV-DJ/2-hSyn1-FRT-dlox-hChR2(H134R)_ EYFP(rev)-dlox-FRT-WPRE-bGHp(A)	Zurich Viral Core	v923-DJ
AAV-hSyn1-SIO-eOPN3-mScarlet-WPRE (AAV1)	Addgene	125713-AAV1
Experimental models: Organisms/strains		
Mouse: LepR-cre (B6.129-Leprtm3(cre) Mgmj/J	The Jackson Laboratory	RRID:IMSR_JAX:032457
Mouse: Vgat-FlpO (B6.Cg-Slc32a1tm1. 1(flpo)Hze/J	The Jackson Laboratory	RRID:IMSR_JAX:02959
Mouse: Vglut2-ires-Cre (Slc17a6 $^{tm2(cre)Lowl/J}$	The Jackson Laboratory	RRID:IMSR_JAX:016963
Mouse: Vgat-ires-Cre (Slc32a1 $^{tm2(cre)Lowl/J}$	The Jackson Laboratory	RRID:IMSR_JAX:016962
Mouse: B6N (C57BL/6N)	The Jackson Laboratory	RRID:IMSR_JAX:005304
Mouse: LepCre mice crossed with Vgat-Flpo mice	Siemens Laboratory	N/A
Software and algorithms		
Prism 8 software	GraphPad Software	https://www.graphpad.com/
Adobe Creative Cloud (Illustrator)	Adobe	https://auth.services.adobe.com/de_DE/deeplink.html
ImageJ software	NIH	https://imagej.net/ij/
IRBIS 3 software	InfraTec	https://www.infratec.de/thermografie/thermografie-software/
Ponemah acquisition software 6.x	Data Sciences International (DSI)	https://www.datasci.com/products/software/ponemah/ponemahV6
Dataquest ART software	Data Sciences International (DSI)	https://www.datasci.com/products/software/dataquest-art
Clampex 11.0.3 software	Molecular Devices	https://support.moleculardevices.com/s/article/Axon-pCLAMP-11-Electrophysiology-Data-Acquisition-Analysis-Software-Download-Page

(*Continued on next page*)

Please cite this article in press as: Bouaouda et al., Thermal-state-dependent control of body temperature and feeding by two intra-hypothalamic pathways, Current Biology (2026), https://doi.org/10.1016/j.cub.2026.01.074

Continued

REAGENT or RESOURCE	SOURCE	IDENTIFIER
Prizmatix Pulser software	Prizmatix	https://www.prizmatix.com/optogenetics/PulserPlus.htm
Other		
Temperature and activity telemetry transmitter	Data Sciences International (DSI)	TA11TA-F10
Arbitrary Function Generator AFG1000	Tektronix	AFG1062
Optogenetics-LED-Blue	Prizmatix	https://www.prizmatix.com/Optogenetics/optogenetics-led-Blue.htm
Blue laser (LRS-0473: 473 nm Blue Laboratory Laser Module)	Laserglow Technologies	LRS-0473-GFM-00100-05
Infra-red camera (VarioCAM®HD head	InfraTec	Serial No: 12656 22

EXPERIMENTAL MODEL AND STUDY PARTICIPANT DETAILS

Transgenic mouse lines

The following mouse lines were used in this study: LepR-cre (B6.129-Leprtm3(cre) Mgmj/J; The 920 Jackson Laboratory, IMSR Cat# JAX:032457), Vgat-FlpO (B6.Cg-Slc32a1tm1.1(flpo)Hze/J Cat# JAX:029591), Vglut2-ires-Cre (Slc17a6 $^{tm2(cre)Lowl/J}$; Jackson Laboratoray, IMSR_JAX 016963), Vgat-ires-Cre (Slc32a1 $^{tm2(cre)Lowl/J}$; Jackson Laboratoray, IMSR_JAX 016962), B6N (C57BL/6N; Jackson Laboratory, IMSR_JAX 005304). By crossing LepR-Cre mice with Vgat-FlpO mice, we generated dual Cre/FlpO transgenic mice that, in combination with a Cre- and FlpO-dependent viral vector, allowed the selective targeting of VMPO vGat-negative or VGat-positive LepR-positive neurons.

Mouse husbandry

Mice of either sex were used in experimental procedures. Mice were housed at room temperature 22–24 °C in air-conditioned lab space / animal vivarium with a standard 12-hour light/dark cycle and *ad libitum* access to food and water. All genetically modified mice in this study were on the C57BL/6N background.

All animal procedures were in accordance with the local ethics committee and governing body (Regierungspräsidium Karlsruhe, Germany) and were approved under protocol numbers: G-168/15, G-169/18, G-181/2, G-97/25 and G-102-25.

Viral AAV constructs

- ssAAV-DJ/2-hSyn1-chI-dlox-ChR2(H134R)_mCherry(rev)-dlox-WPRE-hGHp(A) (titer: 5.3 x 10E12 vg/ml, Zurich Viral Core).
- ssAAV-DJ/2-hEF1α-dlox-ChR2(H134R)_EYFP(rev)-dlox-WPRE-hGHp(A) (titer: 5.5 x 10E12 vg/ml, Zurich Viral Core).
- ssAAV-DJ/2-hSyn1-chI-dlox-mCherry(rev)-dlox-WPRE-hGHp(A) (titer: 7.2 x 10E12 vg/ml, Zurich Viral Core).
- ssAAV-retro/2-shortCAG-dlox-EGFP(rev)-dlox-WPRE-SV40p(A) (titer: 4.3 x 10E12 vg/ml, Zurich Viral Core).
- ssAAV-retro/2-CAG-dlox-tdTomato(rev)-dlox-WPRE-bGHp(A) (titer: 5.1 x 10E12 vg/ml, Zurich Viral Core).
- ssAAV DJ/2-hSyn1-chI-Con/Fon(ChR2(H134R)_EYFP)-WPRE-hGHp(A) (Cre-ON; FlpO-ON expression of ChR2; Zurich Viral Core, titer: 2.7 x 10E12 vg/ml).
- ssAAV-DJ/2-hSyn1-FRT-dlox-hChR2(H134R)_EYFP(rev)-dlox-FRT-WPRE-bGHp(A) (Cre-ON; FlpO-OFF expression of ChR2; Zurich Viral 6.5 x 10E12 vg/ml).
- AAV-hSyn1-SIO-eOPN3-mScarlet-WPRE (AAV1) (Addgene, Catalog # 125713-AAV1).

METHOD DETAILS

Virus injection and optic fiber implantation

Before surgery, 6- to 8-week-old mice were anesthetized using an intraperitoneal (i.p) injection of anesthesia mix (Medetomidine 0.5 mg/kg, Midazolam 5 mg/kg and Fentanyl 0.05 mg/kg). Mice were checked for the absence of the tail-pinch reflex as a sign of sufficient anesthesia. The mice were then immobilized in a stereotaxic frame (Model 1900; Kopf, USA) with ear bars (David Kopf Instruments), and ophthalmic ointment (Bepanthen; Bayer, Germany) was applied to prevent eye drying. The body temperature of animals was kept at 37°C using a heating pad.

After making an incision to the midline of the scalp, small unilateral craniotomies of approximately 0.6 mm diameter were performed with a hand drill (OS40; Osada Electric, Japan). The tips of glass capillaries (20–40 μm tip diameter) loaded with specific recombinant adeno-associated virus (ssAAV) carrying the functional construct or only the fluorescent protein were placed into specific brain areas.

Please cite this article in press as: Bouaouda et al., Thermal-state-dependent control of body temperature and feeding by two intra-hypothalamic pathways, Current Biology (2026), https://doi.org/10.1016/j.cub.2026.01.074

The coordinates for target injection areas included the VMPO (AP, +0.75 mm; ML, −0.2 mm; DV, −4.8 mm from dura), the PVH (AP, −0.6 mm; ML, −0.26 mm; DV, −4.7 mm from dura), the DMH (AP, −1.4 mm; ML, −0.3 mm; DV, −4.9 mm from dura), and the VLPAG (AP, −4.72 mm; ML, −0.5 mm; DV, −2.10 mm from dura), as determined by the mouse brain atlas (Paxinos and Franklin Mouse Brain Atlas, 4th edition). A total of 250 nl of virus-containing solution was injected unilaterally (for optogenetic stimulation experiments) and bilaterally (for optogenetic inhibition experiments) using a manual air pressure system. After injection, the capillary was left in place for an additional 5 min to allow for diffusion of the virus solution and then withdrawn.

Within the same AAV injection session, a 200 μm diameter fiber optic probe (numeric aperture 0.53, Cat# FT200UMT, 1170 ThorLabs) was inserted to target the somas of preoptic LepR, GABA or glutamatergic cells (in VMPO) or terminals (either in the PVH, the DMH, or the vlPAG). The coordinates used for the probe were identical to those used for the AAV injection, except for a 0.4 mm upward adjustment in the dorsal-ventral position to ensure placement of the optic fiber above the area of infection. The probe was anchored to the skull with dental acrylic.

The scalp incision was closed with sterile absorbable-needled sutures (Marlin 17241041; Catgut, Germany), and mice received subcutaneous injection of Carprofen at 5mg/kg (Rimadyl; Zoetis, USA) for pain relief. Subsequently, anesthesia was antagonized with subcutaneous injection of Atipamezole at 2.5 mg/kg, Flumazenil at 0.5 mg/kg, and Naloxon at 1.2 mg/kg. Mice were transferred to their home cages. For postoperative care, a second dose of Caprofen was administered after 24 hours. The mice cages were kept on a veterinary heating pad at 37 °C for 12 hours and closely monitored. A minimum of 4 weeks was allowed for viral expression before any experiments were conducted.

Optogenetic experiments

Optogenetic stimulation experiments were performed in adult LepR-Cre mice, Vgat-Cre mice and Vglut2-Cre mice, at least 4 weeks after AAV injection/implantation procedure.

To activate ChR2-expressing LepR neurons, a fiber optic probe was connected via an FC/PC adaptor to a 473-nm blue LED (Optogenetics-LED-Blue, Prizmatix) or 473-nm blue laser (LaserGlow Technologies, LRS-0473-GFM-00100-05). All ChR2-based experiments were conducted unilaterally, and the fiber optic cable was connected at least 2 hours before the experiments to allow for habituation. During optogenetic probing, mice received light pulses with a power of 4–6 mW, a width of 10 ms, and varying stimulation frequencies (5, 10, 20 Hz) using a Prizmatix Pulser software and pulse train generator (Prizmatix) or signal generator (Tektronix, # AFG1062). Each optogenetic probing session consisted of 1-minute of light stimulation followed by a 3-minute inter-stimulation interval. The optogenetic inhibition of the $VMPO^{LepR}$→PVH and $VMPO^{LepR}$→DMH was triggered via a stimulation protocol using a signal generator (Tektronix, # AFG1062). The blue laser light (473-nm) was transmitted through a fiber optic splitter for bilateral stimulation (FRJ_1x2i_FC-2FC, Doric Lenses, Quebec, QC, canada) to fiber optics cables (1m length, 200μm diameter core, Doric Lenses, Quebec, QC, Canada). The laser power emitted from the tip of the fiber optic cables was measured before and after each stimulation protocol to ensure it was within a range of 500 μW-1 mW. It is important to highlight that this is a high estimate due the light lost at the connection of the fiber optic fiber and the optic fiber cannula. During each opto-inhibition session, the blue laser light (473 nm) was turned on continuously for 4 seconds, then off for 4 seconds. This cycle was repeated for a duration as indicated for the respective experiment.

Following the experiments, each mouse was euthanized (refer to procedure below), and the location of optical implant and viral expression and spread were examined under a fluorescence microscope. Mice with off-target implants, poorly expressed virus, or viral spread to other areas were excluded.

Locomotor activity and temperature recordings

Except for animals designated for electrophysiological recordings, all subjects received an i.p. injection of the anesthesia mix (Medetomidine 0.5 mg/kg, Midazolam 5 mg/kg and Fentanyl 0.05 mg/kg). Following this, the abdominal fur was removed, skin disinfected with Braunol (Cat# 3864065, Braun, Germany), and cornea protected with Bepanthen ointment (Bayer, Germany). An implantable physiological signal wireless telemetry transmitter (TA11TA-F10; Data Sciences International, USA) was implanted in the abdominal cavity of a mouse, after which the muscle and skin layers were sutured separately with absorbable surgical threads (Marlin Cat#17241041, Catgut, Germany). After the surgery, the anesthesia was antagonized with Atipamezole at 2.5 mg/kg, Flumazenil at 0.5 mg/kg, and Naloxon at 1.2 mg/kg. Animals were monitored for recovery as outlined previously; a minimum recovery period of one week was observed before further procedures were undertaken.

The system consists of an implant, a receiver, a data converter (DEM), and a data analysis computer (IRBIS 3 software). The core body temperature signal was converted into a radio signal and received by a receiver (RSC-1, DSI, USA) positioned under the recording cage with a sampling rate of 5 min. Telemetry data were recorded using Dataquest ART and Ponemah 1162 software (DSI, USA).

For measuring tail temperatures and brown adipose tissue temperatures, we employed an infrared thermal camera (Vario CAM, InfraTec, Germany). Snapshot images were taken every 5 min using IRBIS 3 software (InfraTec, Germany). The average temperature was calculated at the midpoint of the tail (segment length of 1 cm) and at the center of the interscapular region, which was shaved 3 days prior to measurements.

Food intake assay

Food intake was assessed over an 11-hour period during the dark phase by quantifying pellet consumption. At the commencement of optogenetic stimulation, each mouse was housed in clear-bottom cages containing pre-weighed mouse chow pellets and a 1-inch layer of fresh sawdust bedding. Optogenetic stimulation was administered in cycles of 1 minute ON followed by 3 minutes OFF, with a stimulation frequency of 10 Hz, spanning an 11-hour duration (from 7 PM to 6 AM). At the end of the stimulation, both the consumed pellet weight and the mouse's body weight were measured.

Fecal corticosterone metabolite measurements

Corticosterone metabolite measurements were carried out on fecal samples as previously described[61] with slight modifications as described in Segeleck et al.[62] In brief, feces were collected from controls (mCherry injected) and ChR2-positive animals around 7AM, directly after the overnight optogenetic stimulation cycle. Fecal boli (5–6 fecal boli per animal) were stored at −20°C. Fecal samples were dried for two hours at 80 °C before mechanical homogenization, and 0.05 g were extracted with 1 ml 80% methanol for 30 min on a vortex. After centrifugation for 10 min at 2500 g, 0.5 ml supernatant was frozen until analysis. Fecal corticosterone metabolite was measured using a 5α-pregnane-3β,11β,21-triol-20-one enzyme immunoassay (EIA).

Electrophysiological recordings

Four weeks after surgery, the mice were deeply anesthetized with Ketamine/Xylaxine mixture (Ketamine: 220mg/kg, Ketavet; Zoetis, USA and Xylazine 16mg/kg, Rompun; Bayer, Germany) and decapitated. Brains were dissected quickly and chilled in ice-cold (4 °C) artificial CSF (aCSF) containing the following (in mM): NaCl, 85; KCl, 2.5; glucose, 10; sucrose, 75; NaH2PO4, 1.25; NaHCO3, 25; MgCl, 3; CaCl2, 0.1; myo-inositol, 3; sodium pyruvate, 2; ascorbic acid, 0.4. Coronal slices (250 μm thick) including the VMPO were prepared using a vibratome (Leica VT1200S, Germany) and then incubated for 7 minutes in heated (32 °C) oxygenated holding aCSF (in mM): NaCl, 109; KCl, 4; glucose, 35; NaH2PO4, 1.25; NaHCO3, 25; MgCl2, 1.3; CaCl2, 1.5. Individual slices were then transferred to the recording chamber where they were continuously superfused with oxygenated recording aCSF at ∼2 ml/min.

Neuronal action potentials in LepR cells were recorded at room temperature in whole-cell current-clamp configuration, with borosilicate glass patch pipette (4–8 MΩ resistance) filled with internal solution containing the following (in mM): K-gluconate, 138; KCl, 1369 2; NaCl, 5; HEPES, 10; EGTA, 10 (or equimolar amount of BAPTA); CaCl2, 1; Mg-ATP, 1. Micropipettes (O.D. 1.5 mm, I.D. 0.86 mm, Sutter Instrument, BF150-86-7.5) were pulled on a micropipette puller (P-97, Sutter Instrument, USA). Intracellular solution was passed through 0.22 μm filter before filling the electrode pipette. The open pipette resistance was between 4-8 MΩ.

Cells in acute VMPO slices were visualized using a SliceScope upright microscope (Scientifica, UK) equipped with a 40X water immersion objective (U-TV1X-2, Olympus, Japan). Images were acquired by a digital CCD camera (ORCA-R2 C10600-10B, Hamamatsu Photonics K.K., Japan) using Micro Manager 1.4 software (Vale's lab, UCSF, USA). Electrophysiological recordings were acquired using a MultiClamp 700B amplifier (Molecular Devices, USA), together with an Axon Digidata 1550B digitizer (Molecular Devices, USA) and Clampex 11.0.3 software (Molecular Devices, USA). All signals were sampled at 20 kHz and low pass filtered at 10 kHz.

To optogenetically stimulate neurons infected with channel-rhodopsin in brain slice preparations containing the VMPO, blue light (470 nm) pulses were applied by a light-emitting diode (LED)-based optical system (pE-100 CoolLed, Scientifica, UK). The target site was illuminated with 10 ms light pulses at variable stimulation frequency (5, 10, and 20 Hz). Each train of the light pulses was given for 60 seconds.

Immunohistochemistry

Mice were anesthetized, transcardially perfused with paraformaldehyde (PFA), and then decapitated. The whole heads were immersed in 4% PFA for at least one day at 4 °C. Subsequentially, the brains were removed from the skull and transferred to a phosphate-buffered saline (PBS) solution containing sucrose. Coronal sections of 30 μm were cut at the microtome and stored at -20 °C in cryoprotectant solution. These brain sections were later stained for GFP, mCherry or dsRed according to the procedure outlined below.

Animals were deeply anesthetized with isoflurane and transcardially perfused with a phosphate buffer solution (PBS; 3.85 g of NaOH and 16.83 g of NaH2PO4 in 1l of distilled water) followed by a 4% paraformaldehyde (PFA) solution. Brains were dissected out and left overnight (O/N) in 4% PFA at 4℃. Over the following 2 days brains were immersed into PBS/sucrose solutions (24 hours in 10% sucrose followed by 30% sucrose, until brains sank to the bottom of container tube). Brains were sectioned with a cryo-microtome at 30 μm thickness and sections (free-floating) were kept in cryo-protectant solution (250 ml glycerol; 250 ml ethylene glycol filled up with PBS to 1L) at 4℃ until mounting. Tissue was washed extensively with PBSX 0.1 and once with PBS after which sections were mounted using Immu-Mount (Cat# 9990402, Fisher Scientific, UK) onto glass slides. Confocal images were taken at the Nikon imaging center at Heidelberg University, with the Nikon A1R confocal microscope under Nikon Plan Apo λ 10x magnification NA 0.45 (working distance 4mm, the field of view 1.27 x 1.27 mm) objective.

Retrograde labelling of LepR neurons

For the retrograde tracing of VMPO LepR neurons, we used the LepR-*Cre* mice and injected the PVH and DMH with retro-AAV (Viral Vector Facility from the University of Zurich; Switzerland) conjugated with Cre-dependent EGFP or tdTomato (see above for specification), respectively (250 nl, unilateral). Confocal microscopic images of the VMPO area were taken at the Nikon imaging center at

Heidelberg University with the Nikon 989 A1R confocal microscope under Nikon Plan Apo λ 10x magnification NA 0.45 (working distance 990 4 mm, the field of view 1.27 x 1.27 mm) objective. For each mouse, images of 3-4 representative fields of the VMPO hypothalamic area were acquired. Double-projecting VMPO neurons were identified based on cell bodies labeled with both tdTomato and EGFP. The proportion of double projecting VMPO neurons to VMPO neurons projecting to either the PVH or DMH was also calculated for each mouse. Images presented were processed with ImageJ.

QUANTIFICATION AND STATISTICAL ANALYSIS

Statistical analysis was performed using GraphPad Prism 8 (GraphPad Software, San Diego, CA). Data were expressed as mean ± SEM and were analyzed using one-way, two-way ANOVA, and t tests (two-tailed) as indicated. Fisher, Tukey or Dunnett's multiple comparisons test was used as post hoc comparisons of ANOVA. A value of $p<0.05$ was considered statistically significant.